



HAL
open science

Effects of soil process formalisms and forcing factors on simulated organic carbon depth-distributions in soils.

Saba Keyvanshokouhi, Sophie S. Cornu, Francois Lafolie, Jérôme Balesdent, Bertrand Guenet, Nicolas Moitrier, Nathalie Moitrier, Cédric Nouguier, Peter Finke

► To cite this version:

Saba Keyvanshokouhi, Sophie S. Cornu, Francois Lafolie, Jérôme Balesdent, Bertrand Guenet, et al.. Effects of soil process formalisms and forcing factors on simulated organic carbon depth-distributions in soils.. Science of the Total Environment, 2019, 652, pp.523-537. 10.1016/j.scitotenv.2018.10.236 . hal-01904523

HAL Id: hal-01904523

<https://hal.science/hal-01904523v1>

Submitted on 3 May 2019

HAL is a multi-disciplinary open access archive for the deposit and dissemination of scientific research documents, whether they are published or not. The documents may come from teaching and research institutions in France or abroad, or from public or private research centers.

L'archive ouverte pluridisciplinaire **HAL**, est destinée au dépôt et à la diffusion de documents scientifiques de niveau recherche, publiés ou non, émanant des établissements d'enseignement et de recherche français ou étrangers, des laboratoires publics ou privés.

1 **Effects of soil process formalisms and forcing factors on simulated organic carbon**
2 **depth-distributions in soils**

3

4 Keyvanshokouhi, S.^{a,b}, Cornu, S.^a, Lafolie, F.^c, Balesdent, J.^a, Guenet, B.^d, Moitrier, N.^c,

5 Moitrier, N.^c, Nougier, C.^c, Finke, P.^b

6

7 a- Aix-Marseille Univ, CNRS, IRD, INRA, Coll de France, CEREGE, 13545 Aix en
8 Provence, France

9 b- Ghent University, Department of Environment, Coupure Links 653, B-9000,
10 Belgium

11 c- EMMAH, INRA, Université d'Avignon et des Pays de Vaucluse, 84000 Avignon,
12 France

13 d- Laboratoire des Sciences du Climat et de l'Environnement (LSCE/IPSL), UMR8212
14 (CEA-CNRS-UVSQ), Université Paris-Saclay, 91198 Gif-sur-Yvette Cedex, France

15

16

17 **Abstract**

18 Soil organic carbon (OC) sequestration (i.e. the capture and long-term storage of
19 atmospheric CO₂) is being considered as a possible solution to mitigate climate change,
20 notably through land use change (conversion of cropped land into pasture) and
21 conservation agricultural practices (reduced tillage). Subsoil horizons (from 30 cm to 1
22 meter) contribute to ca. half the total amount of soil OC, and the slow dynamics of deep OC
23 as well as the relationships between the OC depth distribution and changes in land use and
24 tillage practices still need to be modelled.

25 We developed a fully modular, mechanistic OC depth distribution model, named OC-VGEN.
26 This model includes OC dynamics, plant development, transfer of water, gas and heat,
27 mixing by bioturbation and tillage as processes and climate and land use as boundary
28 conditions. OC-VGEN allowed us to test the impact of 1) different numerical
29 representations of root depth distribution, decomposition coefficients and bioturbation; 2)
30 evolution of forcing factors such as land use, agricultural practices and climate on OC
31 depth distribution at the century scale.

32 We used the model to simulate decadal to century time scale experiments in Luvisols with
33 different land uses (pasture and crop) and tillage practices (conventional and reduced) as
34 well as projection scenarios of climate and land use at the horizon of 2100. We showed
35 that, among the different tested formalisms/parametrizations: 1) the sensitivity of the
36 simulated OC depth distribution to the tested numerical representations depended on the
37 considered land use; 2) different numerical representations may accurately fit past soil OC
38 evolution while leading to different OC stock predictions when tested for future forcing
39 conditions (change of land use, tillage practice or climate).

40

41 **Keywords**

42 Climate change, pasture, reduced tillage, organic matter, OC projection, model formalisms

43 1. Introduction

44 Soil organic matter is the largest terrestrial carbon reservoir that is in constant
45 exchange with the atmosphere and, consequently, a small change in this carbon reservoir
46 can have a strong effect on atmospheric CO₂. Estimating the response of soil organic
47 carbon (OC) to climate change is crucial (Smith et al., 2008; Minasny et al., 2017) because
48 soil OC sequestration is being considered as a possible solution to mitigate climate change,
49 converting atmospheric CO₂ into long-life soil organic carbon. Land use change
50 (conversion of cropped land into pasture) and conservation agricultural practices
51 (reduced tillage), considered as a strategy to sequester carbon in soil, have been
52 extensively studied (Paustian et al., 1997; Jobbágy and Jackson, 2000; Post & Kwon, 2000;
53 Lal, 2004). Nevertheless, the relationship between the OC depth distribution and changes
54 in land use and tillage practices is still poorly understood (Jobbágy and Jackson, 2000;
55 Lorenz and Lal, 2005) and controversial results have been reported concerning the effects
56 of tillage reduction (Haddaway et al., 2016).

57 Thus, there is an urgent need to better predict the OC stock evolution under land use,
58 management and climate change scenarios by the year 2100. Heretofore, most predictive
59 modelling efforts (Smith et al., 2005; Xu et al., 2011; Lugato et al., 2014; Wiesmeier et al.,
60 2016) concentrated on the upper 30 cm of soil, e.g. those based on RothC (Coleman et al.,
61 1997) or Century (Parton, 1996). These models describe OC as an ensemble of organic
62 pools with different decay dynamics, but do not consider other soil processes or depth
63 distributions. However, while the upper 30 cm (topsoil - A Horizon) of soil profile
64 represents the highest organic matter concentrations, recent studies show that subsoil
65 horizons (from 30 cm to 1 meter) contribute to 30 to 63 % of the total amount of soil OC
66 (Batjes, 2014). Consequently, OC stock prediction must not be restricted to the upper 30
67 cm of the soil but should also consider deep OC stocks. Indeed, Balesdent et al. (2018)
68 indicated that "using multilayer soil modules in global carbon models could help to
69 improve our understanding of soil-atmosphere carbon exchange".

70 However, deep OC dynamics is generally not considered in OC modelling approaches or
71 only to a limited extent (Nakane, 1978; Elzein and Balesdent, 1995; Baisden et al., 2002;
72 Guenet et al., 2013) because the transport mechanisms of OC into deep layers are not well
73 understood. Indeed, their direct measurement of deep OC evolution is limited due to very
74 low concentrations and very slow changes. Information on contribution of deep roots to
75 OC stock is rarely available while obtaining data on deep OC decomposition is not possible
76 without disturbing the processes involved. Therefore, these processes may be addressed
77 either by using tracers as stable C isotopes (Balesdent et al., 2018) or by modelling
78 approaches. Recent works emphasized the need for multilayer soil carbon modules
79 (Campbell and Paustian, 2015; Luo et al., 2016). He et al. (2016) suggested that Ecological
80 Soil Models "must better represent carbon stabilization processes and the turnover time of
81 slow and passive reservoirs when simulating future atmospheric carbon dioxide
82 dynamics";

83 The processes responsible for deep OC stock change are transport of dissolved OC,
84 bioturbation, root input and decomposition. Several attempts were made to introduce
85 these processes in OC dynamic modelling. (e.g., Hilinski, 2001; Braakhekke et al., 2011;
86 Koven et al., 2013; Riley et al., 2014; Camino-Serrano et al., 2018). Nevertheless, for these
87 key processes, several numerical representations (including the equations and
88 parametrization) exist in the literature (e.g. Elzein and Balesdent, 1995; Jackson et al.,
89 1996; Zeng, 2001; Koven et al., 2013 among others), and are often model-specific. The
90 impact of these different numerical representations on the simulated OC depth-
91 distribution should be evaluated. But because of model-specific formalisms, it is difficult to
92 modify their parameterization because of their imbrication with the parameters of other
93 processes.

94 In addition, at the century scale, when considering climate change 1) explicit transfer of
95 water and heat should be considered and 2) inherent soil properties that are important for
96 OC dynamic, as soil texture, bulk density and hydraulic properties, cannot be considered

97 constant (e.g. Montagne et al., 2008; Boizard et al., 2013). As an example, soil OC content is
98 related to the soil bulk density, which influences soil hydraulic properties and thus soil
99 water content that in turn affect the OC decomposition. Because deep OC might be
100 thousands years old and interacts dynamically with soil development, OC dynamics must
101 be coupled with a model of pedogenesis. Therefore, the retroaction among soil properties
102 much be taken into account explicitly.

103 Based in this analysis, we developed a fully modular OC depth distribution model, called
104 OC-VGEN that provides a multilayer representation of the soil; takes into considerations
105 among soils properties while modelling OC dynamics; allow considering landuse and
106 tillage practices as well as most of the depth distribution processes considering their
107 different formalisms.

108 The motivations for the development of OC-VGEN are not to add one model to the long list
109 of existing soil C models (Campbell and Paustian, 2015), but to be able to test alternate
110 formalisms for a given process. Hereto, we build OC-VGEN in a modular platform VSoil
111 (Lafolie et al., 2014), that allows easy coupling of OC dynamics with other processes of soil
112 development that interact with OC itself through feed-back loops, such as bioturbation or
113 changes in soil chemistry, granulometry, porosity and hydraulic properties. Such model
114 will allow users to identify where uncertainty about process formulations impacts the
115 accuracy of relevant model outputs (such as OC depth distribution and its change over
116 time), and thus, where more research is needed before OC-modelling can be successful
117 and accurate.

118 OC-VGEN was then used to test the impact of 1) different numerical representations of
119 root depth distribution, OC decomposition coefficients and vertical transfer by
120 bioturbation; 2) forcing factors such as land use, agricultural practices and climate on OC
121 depth distribution at the century scale. Therefore, the model was tested on long-term
122 experiments on Luvisols that includes different land uses (pasture and crop) and tillage

123 practices (conventional and reduced) and was forced by projection scenarios of climate
124 and land use at the horizon of 2100.

125

126 2. Materials and Methods

127 2.1 Description of OC-VGEN model and its variations

128 OC-VGEN is a pedon scale, mechanistic model that takes into account factors of soil
129 formation (climate, organisms, relief, parent material and human activities on soil) as
130 initial or boundary conditions. It focuses on carbon dynamics and was developed in the
131 VSoil modelling platform (Lafolie et al., 2014; Brimo et al., 2018). Other processes are
132 fluxes of water, gas and heat, solid mixing processes such as bioturbation and tillage as
133 well as plant development (Table 1 and Figure 1).

134

135 2.1.1 The VSoil platform

136 VSoil (Lafolie et al., 2014; Brimo et al., 2018) is a component-based platform that
137 aims at designing, developing and implementing bio-geochemical and physical processes
138 in soil. There is clear distinction in this platform between knowledge defined as *processes*
139 and their mathematical representation defined as *modules*. Processes of any kind
140 (physical, chemical, biological) influencing soil properties occurring within soil or at its
141 boundaries (atmosphere and water table) can be described. Several numerical expressions
142 and computer codes (modules) can be proposed to represent each of the processes. The
143 modules associated to one process can differ by their numerical representations having
144 different levels of complexity (from fully mechanistic to empirical), or by the numerical
145 technique used to solve the equations or by the programming language (FORTRAN or
146 C++). The processes and the associated modules can represent an actual process
147 happening in the soil or an equation that leads to the evolution of soil properties. For
148 example, the dynamic estimation of soil hydraulic properties and mass balance equations
149 are defined as processes.

150 To build a model, a set of processes is selected, each process being associated to a module.

151 The platform makes the connection between the processes/modules according to the

152 defined input and outputs. Alternative versions of a same model can be designed by
153 changing the modules associated to one or more processes of that model. In this paper we
154 developed the OC-VGEN model in the VSoil platform as well as alternative versions of it by
155 changing one module at a time as described below.

156

157 2.1.2. Simulation protocol

158 The impact of different numerical representations and parameters of plant rooting depth
159 distribution, bioturbation and depth-dependent decomposition rate coefficient on the OC
160 depth distribution was analyzed by running the model, changing one formalism
161 (numerical representation or parameter) for each run. Table 2 summarizes the 6
162 formalisms: one reference run, three alternative formalisms for rooting depth (Alt1-
163 RD_Jackson, Alt2-RD_Zeng, Alt3-RD_A/B, see also section 2.1.5), one alternative formalism
164 for a depth-dependent decomposition coefficient (Alt4-OC_DDCoeff, see also section 2.1.3)
165 and one alternative formalism for bioturbation (Alt5_Bioturb, see also section 2.1.6).
166 These alternatives were performed for three different land use/agricultural practices
167 known to affect OC in soil, namely cultivation with conventional tillage (M1) or reduced
168 tillage (M2) and pasture (M3) for one site (Mons; Table 3, see also section 2.2.1). This
169 made a total of 18 simulations (6 models run for 3 land use/practices - Table 2)
170 representing the past until 2011 AD.

171 More specifically, for each simulation, a warming run (spin-up) was designed to simulate
172 the initial state of the system. The spin-up runs consisted in a 300 years simulation except
173 for the OC_DDCoeff version of the model for which the spin-up duration was extended to
174 1000 years. This was done because after 300 years, this model version still showed
175 dependency of the initial situation. IOM was fixed as equal to the concentration of C
176 horizon (105-125 cm). Then 1939-2011 scenarios were simulated for cultivation with
177 conventional tillage, reduced tillage and pasture starting with the respective steady state

178 obtained by the corresponding version of the model. Climatic condition for these runs are
179 reported in Figure 2.

180 The impact of future climate change at horizon of 2100 was then analyzed based on 6
181 climatic scenarios (RCP2.6 and RCP8.5, each simulated by 3 climate models HadGEM, IPSL-
182 CM5A and MIROC-ESM-CH, see Figure 3) for the three considered land use/tillage
183 practices and the 6 considered model versions. This resulted in 108 additional
184 simulations. These runs were designed as continuations of the previous one. Therefore, no
185 spin-up steps were run for equilibration purposes.

186 The over-all layout of these simulations is shown in Figure 4.

187

188 2.1.3. Description of the OC-VGEN modules

189 2.1.3.1 The OC dynamic module

190 The OC dynamic module was developed based on the Rothc-26.3 model (Coleman et al.,
191 1997) with some adaptation based on SoilGen (Finke and Hutson, 2008). In this model,
192 fresh organic matter input is split between different pools (decomposable plant material
193 (DPM), resistant plant material (RPM), biomass (BIO), humus (HUM), inert organic matter
194 (IOM), Figure 1). Organic matter decomposes over time with half-life that differs strongly
195 among pools (a month for DPM; one to three years for BIO, three to ten years for RPM,
196 over 50 years for HUM, IOM is considered as stable in the model; Janik et al., 2002).
197 Decomposition rates additionally depend on moisture deficit, temperature, soil cover and
198 texture (Equation 1).

$$K(z) = K_{0,p} r_T(z) r_{Wt}(z) r_{SC}(z) r_z(z) \quad (1)$$

199 Where $K(z)$ is the pool- and depth-dependent decomposition rate, $K_{0,p}$ is the pool
200 dependent decomposition rate coefficient which is constant over depth and r , are the rate
201 modifiers corresponding to T , the soil temperature calculated by the heat transfer module,
202 SC , the soil cover, and Wt , both the moisture deficit and the $< 2 \mu\text{m}$ fraction. The term $r_z(z)$

203 represents other depth dependent processes such as priming effect, i.e. the reduction of
204 decomposition rates at depth as a result of low fresh substrate supply (Guenet et al., 2013;
205 Shahzad et al., 2018). Koven et al. (2013) proposed an exponential function for $r_z(z)$, that
206 decreases with depth to account for those processes (Equation 2).

$$r_z(z) = \exp\left(\frac{-z}{z_\tau}\right) \quad (2)$$

207 where z_τ is the e-folding depth of the intrinsic decomposition rates. This depth was
208 optimized by Koven et al. (2013) to 40 cm.

209 Temperature, moisture deficit and $< 2 \mu\text{m}$ fraction are also depth dependent and are
210 calculated using the same equations from the RothC26.3 model (Jenkinson and Coleman,
211 2008)

212 Soil moisture deficit corresponds to the difference between potential evapotranspiration
213 and precipitation, being vertically distributed according to air filled porosity depth profile
214 derived from the water transfer module.

215 At last, the partition coefficient among RPM/DPM pools in litter (the only pools
216 represented in litter) is a function of the vegetation type/land use.

217 This module was implemented in VSoil platform as a core of OC-VGEN model to account
218 for the dynamics of organic carbon in soil and used with $r_z(z)$ equals to one except for one
219 simulation in which the impact of the decomposition coefficient formalism on OC depth
220 distribution is evaluated (the scenarios are summarized in Table 2). While in the A
221 horizon, the OC decomposition rate corresponds to that calibrated in SoilGen, it decreases
222 exponentially below that horizon.

223

224 2.1.3.2. Water, heat and gas transfer modules

225 OC-VGEN uses Richard's equation to simulate the flow of water and advection-diffusion
226 equations to model flow of heat and gas. A central-difference Crank-Nicholson approach is

227 used to solve transport equations. It was developed after Pastis (Cannavo et al., 2006).
228 Upper boundary conditions in water module allow for surface infiltration, evaporation and
229 zero flux, while the lower boundary accounts only for free drainage in this study. When the
230 soil infiltrability is exceeded, a water runoff module simply returns a soil surface potential
231 to zero. Additionally, the soil cover fraction limits the evaporative flux at the upper
232 boundary. This fraction is a function of the vegetation.

233 Soil hydraulic properties are simulated by the model once a year by the Hypress
234 pedotransfer function based on the texture, OC and the bulk density (Wösten et al.,1999;
235 adapted by Finke, 2012). Soil bulk density, water content and porosity are used to
236 calculate soil heat capacity and thermal conductivity. Diffusive heat flux and transport by
237 water are simulated.

238

239 2.1.3.3. Plant development modules

240 The plant development modules aim at bringing organic carbon into soil and up taking
241 water from it. They consist in two modules: a plant development module and a module of
242 water uptake by roots (Figure 1).

243 The plant development module provides organic matter input and root distribution
244 profile. The organic matter input to soil consist in an input file indicating OC input through
245 Net Primary Production (NPP) or/and organic amendments. This input is subsequently
246 split between the above and below ground pools. Both pools then decay over time with
247 similar equations as described in organic matter dynamic module. The ratio of above to
248 below ground fresh organic input and the DPM/RPM ratio depend on the vegetation
249 type/land use.

250 The plant root depth distribution is defined by a root density function and a rooting depth.
251 The first consist in the formalism of root depth distribution while the latter is a parameter
252 of that formalism.

253 Generally, in literature the root depth distribution formalism is represented by an
254 exponential equation, with some variations among authors. OC-VGEN originally uses
255 Equation 3 for permanent vegetation considering a steady rooting profile.

$$RDF(z) = \alpha \cdot e^{-\alpha z} \quad (3)$$

256 where, RDF ($m_{\text{root}} m^{-3}_{\text{soil}}$) is the root density function calculated for each compartment
257 inside the maximum rooting depth, z , represents the depth (m) and α is equal to $4 m^{-1}$
258 based on Finke (2012).

259 Davidson et al. (1978) proposed a root density function for crops in which the root is
260 assumed to be growing within the year based on the pre-defined dates of planting,
261 germination and root maturity according to Equation 4.

$$RDF(z, t) = R_{max}(t) \exp(-\beta z^2) \cos \frac{\pi z}{2L(t)} \quad (4)$$

262 in which, R_{max} is the maximum root density at $z=0$, z is the soil depth and L is the depth of
263 the bottom of root zone, and β is an empirical function of the number of days since
264 planting up till root maturity, originally developed for corn crops. At harvest, plant roots
265 are no longer active regarding the uptake of water from the soil. For more details, see
266 Davidson et al. (1978). This approach was used in OC-VGEN as used previously in the
267 SoilGen model (Finke, 2012) for crops.

268 On the other hand, Jackson et al. (1996) fitted the function developed by Gale and Grigal
269 (1987) to a global data set of root profile measurements and reached a global average
270 rooting distribution function (Equation 5) that is common for the different plant groups
271 (grass, shrubs, crop, trees).

$$RDF(z) = -\ln(\beta) \cdot \beta^z \quad (5)$$

272 where, β is the depth coefficient estimated by fitting to the measured data for each
273 vegetation type. β is equal to 0.943 and 0.961 with $r^2=0.88$ and 0.82 for pasture and crop
274 respectively.

275 Zeng (2001) fitted a double exponential equation (Equation 6) on the rooting depths
276 reported by Canadell et al. (1996). This equation is an improved version of Jackson et al.
277 (1996).

$$RDF(z) = \frac{1}{2}(a \cdot e^{-az} + b \cdot e^{-bz}) \quad (6)$$

278 with a equals 10.74 and 5.558 m^{-1} , and b , 2.608 and 2.614 m^{-1} , for pasture and crop
279 respectively.

280 The parametrizations for rooting depths result in three different root depth distribution
281 formalisms (Table 2). These formalisms include different choices for the distribution of
282 fresh organic matter over the litter layer (aboveground) and rooted layers (belowground),
283 which are expressed by above/below ground ratios (Table 2). . The two alternative
284 formalisms (Jackson et al., 1996; Zeng, 2001) and the corresponding parametrizations
285 were implemented in VSoil platform to create three alternative model versions
286 (RD_Jackson, RD_Zeng and RD_A/B – summarized in Table 2). Note, that in all the above
287 cases RDF is scaled to sum to 1 over the rooted zone.

288 Lastly, root water uptake calculation, a sink term in Richard's equation, is based on
289 LEACHC (Hutson, 2003). This function optimizes the root water potential to minimize the
290 difference between the transpiration demand and the flux of water from the soil to the
291 roots taking into account the fraction of active roots present, the soil-water matrix
292 potential (m) and hydraulic conductivity ($m \ s^{-1}$) at each soil layer. The transpiration
293 demand is calculated from the potential evapotranspiration and the vegetation
294 development provided by the crop development module.

295

296 2.1.3.4 Mass mixing modules

297 Mass mixing processes considered in OC-VGEN are bioturbation and tillage.

298 Bioturbation is classically described in the literature based on the diffusion equation
299 (Elzein and Balesdent, 1995; Jarvis et al., 2010; Tonneijck et al., 2016).

$$\frac{\partial M_{OC}(z, t)}{\partial t} = D(z) \frac{\partial^2 M_{OC}(z, t)}{\partial z^2} \quad (7)$$

300 while $D(z)$ is the diffusion coefficient and M_{OC} , the organic carbon mass. $D(z)$ has been
301 classically considered as constant through depth. Nevertheless, Jagercikova et al. (2014)
302 recently introduced the depth-dependent diffusion coefficient that exponentially
303 decreases in depth (Equation 8).

$$D(z) = D_0 e^{-bz} \quad (8)$$

305 where D_0 is the diffusion coefficient at the surface ($\text{m}^2 \text{s}^{-1}$) and b , the parameter of
306 exponential decrease (m^{-1}).

307 Jagercikova et al. (2014), fitted Equation 8 to ^{137}Cs activities measured on the long-term
308 experiment site considered in this study and obtained the following values of D_0 and b for
309 the pasture profile: $D_0 = 5.42 \pm 1.81 \text{ cm}^2 \text{ yr}^{-1}$ and $b = 0.04 \pm 0.01 \text{ cm}^{-1}$. No ^{137}Cs was
310 detected below 50 cm suggesting a negligible bioturbation below that depth.

311 A different modelling approach for bioturbation, was introduced in SoilGen2.24 model
312 (Finke, 2012). In this approach a portion of each soil layer is distributed vertically among
313 the other soil layers of the bioturbated depth and then homogenized with the remaining
314 soil in each layer to predict the soil properties at each compartment after the process of
315 vertical mixing. The mixing proportions per layer and the mixing depths are yearly model
316 inputs.

317 Both formalisms include the redistribution of both soil solid and liquid phases. OC-VGEN
318 originally uses the approach used in SoilGen2.24. In addition, the diffusive bioturbation is
319 implemented in the VSoil platform as an alternative to allow for evaluation of the impact
320 of bioturbation formalism on OC depth distribution (the alternative model created using
321 this module is called Bioturb and is summarized in Table 2).

322 Tillage was implemented after SoilGen2.24 (Finke, 2012). In this model, as for
323 bioturbation, a portion of each soil compartment is distributed vertically among the other
324 soil layers of the tilled depth and then homogenized with the remaining soil in each layer
325 to predict the soil properties at each layer after the process of vertical mixing. A mixing
326 proportion per layer and the tilled depths are defined by the user and can vary over time.

327

328 2.1.3.5. The mass balance process

329 A mass balance process was introduced in OC-VGEN to account for the changes applied to
330 soil OC and soil particles mass fraction (clay, sand and silt) through different processes. In
331 this approach the model does not exchange the value of each property (X), but the changes
332 applied, $\Delta p(X)$, during the time increment, to that property X by a given process p . Each
333 process will produce a $\Delta p(X)$ which is an input of the mass balance process. The mass
334 balance process will update the mass of X , M_X , and provide the new value whenever it is
335 needed. The module associated to this process is based on equation 9.

$$M_X(t + 1) = M_X(t) + \sum_{p=1}^n \Delta_p(M_X) \quad (9)$$

336 where, t represents the time step and n , number of processes modifying X .

337

338 2.1.4. OC-VGEN input data requirements, time step and depth discretization

339 OC-VGEN needs as initial conditions the characteristics of soil corresponding to the
340 distribution of different particle sizes (clay, sand and silt), OC content, bulk density and
341 water content and as boundary conditions the yearly time series of temperature,
342 precipitation and corresponding evapotranspiration as well as land use and vegetation
343 from the four existing land use/vegetation types (agriculture, pasture, coniferous and
344 deciduous woodland).

345 The time step of the model varies from a few seconds for the case of simulations of water
346 flow, to a day for simulation of OC dynamics, or to a year for application of tillage and
347 bioturbation.

348 The soil profile is discretized on layers of thickness ranging from few millimeters to few
349 centimeters. In this study we used a fixed layer thickness of 0.05 m down to 1.2 m depth.

350

351 2.2 Evaluation data set, forcings and statistical analyses

352 2.2.1. Evaluation data set

353 The evaluation dataset consists in soil characteristics collected on three Luvisol plots from
354 a long-term experiment on a Loess deposit, in the Paris Basin, at Mons. All plots were
355 cropped 260 years before present as shown on Cassini maps (Cassini, 1750). Seventy-two
356 years before the sampling date, one of the plots was converted to pasture while the other
357 two experienced differentiated tillage: one plot continued with conventional tillage, the
358 other experienced reduction in tillage depth and intensity over the last 10 years (Table 3).
359 Soil profiles were already extensively characterized by Jagercikova et al. (2014).

360

361 2.2.2. Forcing data set

362 Forcing data consist in climate, NPP, land use and tillage history.

363 For the spin-up runs, forcing data consist in input fluxes and climate of 1939-1958 period
364 and cultivation with conventional tillage as a land use (Figure 2).

365 For the 1939-2011 period, forcing data consisted in the land use history of the three above
366 described plots. OC inputs are known for the last 10 years for the two-cropped plots and
367 estimated at 5 until 1970 and then at 4 t ha⁻¹ yr⁻¹ from 1970 to 2001 (Figure 2c). This
368 decrease in OC inputs was due to an increase of the crop exportation with agriculture

369 intensification in the 70's. For the pasture, they were estimated at 6.7 t ha⁻¹ yr⁻¹ based on
370 the annual yields estimated by the technical institute for pasture in this region of France.
371 Climate input data were provided by Meteo France for this site (SAFRAN grid; Quintana-
372 Seguí et al., 2008) for the period extending from 1939 to 2011 (Figure 2).

373 For the 2011-2100 period, two economic scenarios were considered, the RCP 2.6
374 (greenhouse emissions decreasing after 2020) and RCP8.5 (emissions continue to rise)
375 IPCC scenarios (Vuuren et al., 2011). We used as input climate the bias-corrected outputs
376 produced within the ISI-MIP project (Warszawski et al., 2014) from three Earth System
377 Models (ESM) named the HadGEM, IPSL-CM5A and MIROC-ESM-CH for these two
378 scenarios (Figure 3a, b and c). The NPP was estimated by running the land surface model
379 ORCHIDEE (Krinner et al., 2005) forced by the climate fields of the three ESMs for the two
380 scenarios (RCP 2.6 and RCP8.5). The precipitation variations range from -20 to +50 mm,
381 temperature rise from 2 to 8 ° C and NPP increase from 1 to 2.4 (t C ha⁻¹) depending on
382 the considered scenario and on the selected ESM.

383 2.3 Data treatment

384 In order to estimate the impact of formalisms of the three selected processes (root depth
385 distribution, bioturbation and OC depth decomposition) on OC depth distribution we
386 compared, the OC stocks simulated using different formalisms at the end of the simulation.
387 Comparisons are presented in terms of percentage of variations, ΔOC , calculated in
388 Equation 10.

$$\Delta OC = 100 \times \frac{OC_{Alt} - OC_{Ref}}{OC_{Ref}} \quad (10)$$

389 where OC_{Ref} stands for OC stock in mineral horizons simulated using the reference setting
390 of process formalism in OC-VGEN model (Ref in Table 2) and OC_{Alt} , the OC stock simulated
391 by model versions built based on alternative formalisms (Table 2). Permanent above
392 ground OC layer (ectorganic) when existing (pasture) is considered in the total soil OC
393 stock calculation, but not in OC depth distribution analysis as this layer is not considered

394 to be in the soil profile. We specifically looked into deep OC stocks response to different
 395 formalisms or parameters. Below 30 cm, OC stocks are considered as deep OC in this
 396 study.

397 We also compared the OC stocks simulated by the different versions of the model to
 398 measurements made on the long-term experiment plots to test the quality of the different
 399 version of the model. We estimated the model–measurement discrepancy using statistics
 400 of deviation as proposed by Kobayashi and Salam (2000).

401 The Mean Squared Deviation, MSD (Equation 11) was calculated as well as its three
 402 components, being: the squared bias of simulation (Equation 12), the squared difference
 403 between standard deviations of simulation and measurements (SDSD – Equation 13) and
 404 the lack of positive correlation weighted by the standard deviations (LSC – Equation 14).

$$405 \quad MSD = \frac{1}{n} \sum_{i=1}^n (x_i - y_i)^2 = (\bar{x} - \bar{y})^2 + \frac{1}{n} \sum_{i=1}^n [(x_i - \bar{x}) - (y_i - \bar{y})]^2 \quad (11)$$

$$406 \quad SB = (\bar{x} - \bar{y})^2 \quad (12)$$

$$407 \quad SDSD = (SD_s - SD_m)^2 \quad (13)$$

408 where SD_s is the standard deviation of simulations and SD_m that of measurements.

409 And finally,

$$410 \quad LSC = 2SD_s SD_m (1 - r) \quad (14)$$

411 Where r represents the correlation coefficient between the simulations and measurements
 412 being:

$$413 \quad r = \frac{\frac{1}{n} \sum_{i=1}^n (x_i - \bar{x})(y_i - \bar{y})}{SD_s SD_m} \quad (15)$$

414 The sum of the three component equals the MSD by definition. The lower the value of MSD,
 415 the closer the simulation is to the measurement.

417 3. Results and discussion

418 3.1 Impact of formalism of key OC depth distribution processes

419 Simulated total soil OC stocks were as expected affected at the first order by the
420 introduction of a depth-variable decomposition rate coefficient or by a change in the
421 above/below ground fresh organic input for pasture. Other changes in the numerical
422 representation of the processes only affected the OC depth distribution within the soil
423 profile (Table 4). While considering the deep OC stocks (30-120 cm), the introduction of a
424 depth-variable decomposition rate coefficient resulted in an increase of those stocks while
425 other numerical representation changes decreased them (Table 4). While considering the
426 depth distribution in more details (Figure 5), the effect of the different numerical
427 representation of the processes was more complex as described below.

428 ***Effect of the root density function*** - In comparison to default rooting function and for the
429 two cropped profiles, the use of Zeng (2001) and Jackson et al. (1996) formalisms
430 increased the OC stocks simulated for the upper soil layers (0 to 35 cm) by 20 % and
431 decreased it below 40 cm, with maximum decrease of 20% around 60 cm (Figure 5 a and
432 b). Zeng (2001) formalism produced slightly higher OC stocks than Jackson et al. (1996)
433 formalism below 70 cm. For pasture, both functions increased the OC stocks above 15 cm
434 depth, with an increase of 20 % for the first soil compartment. This increase was larger
435 and deeper (up to 25 cm) with Jackson et al. (1996) than with Zeng (2001) formalism.
436 Below that depth, both formalism simulated lower OC stocks than the formalism used as a
437 reference (Finke, 2012). When considering Zeng (2001) formalism, this decrease occurred
438 mainly from 15 to 70 cm in depth with a maximum decrease of 10 % around 25 cm, while
439 with Jackson et al. (1996) formalism, the decrease started from 25 cm depth with a
440 maximum of 10 % around 50 cm. In the case of Zeng (2001) formalism, no differences in
441 OC stocks compared to the reference function were recorded below 70 cm (Figure 5b).

442 ***The use of conventional diffusive transport of OC for bioturbation*** instead of a vertical
443 mixing of matter (based on SoilGen2.24, Finke, 2012) increased the OC stocks between 45

444 and 110 cm depth, with a maximal decrease at 50 cm (by about 20 %), for the three
445 considered plots. For the surface layers (0-40 cm), the impact of the use of conventional
446 diffusive transport of OC by bioturbation instead of a vertical mixing of matter differed
447 between land uses. For agriculture, a OC stock decrease of 5 to 15 % was simulated, while
448 for pasture, this stock was decreased by 30 % for the upper soil layer and then was
449 increased between 10 and 20 by as much as 5 % (Figure 5c).

450 ***Effect of the above/below ground ratio of fresh organic carbon input*** - For pasture, the
451 alternative scenario corresponded to an increase of the below ground contribution while
452 for agriculture it corresponded to a decrease. In the case of pasture, increasing the below
453 ground contribution logically increased the OC stocks over the whole soil profile by 15 to
454 50 % depending on the considered depth (Figure 5d), with a maximum increase round 10
455 cm. The total soil OC stocks increased by 23% while the ectorganic layer decreased by
456 60% (Table 4). For agriculture, reducing the below ground input did not affect the total
457 soil OC stock (Table 4) since both above and below ground inputs are mixed by tillage.
458 However, it increased the OC input to the soil in the tillage layer and conversely decreased
459 the soil OC input by roots. Therefore, a decrease of the OC stock below 40 cm was
460 observed. This decrease was maximal around 50 cm, where the root proportion was still
461 important, and it became lower below that depth as the root abundance decreased. Above
462 40 cm, the OC stocks increased by 15 % on the entire depth interval for the conventional
463 tillage and by 40 % over the 10 upper centimetres for the reduced tillage plot (Figure 5d).

464 ***The introduction of a depth-variable decomposition rate coefficient*** only influenced the
465 OC depth distribution below 30 cm since the decomposition rate coefficients used above
466 that depth were the same in the reference and OC_DDcoeff models. The exponential
467 decrease with depth of the decomposition rate coefficient increased as expected the OC
468 stocks up to 85 % at around 100 cm depth for all the considered land uses and tillage
469 practices (Figure 5e). Below the bioturbation depth (i.e., 50 cm), models that combine an
470 exponential decrease with depth of both root input ($\exp(-\alpha z, \text{Eq.3})$) and decay rates ($\exp(-\zeta z,$

471 Eq. 2) result in equilibrium carbon profile following the shape of $\exp(-\alpha + \zeta)z$. The C
472 profile is further influenced by the variation in soil moisture and clay content of the
473 horizons, and the increasing proportion of IOM. In the studied soils, the parameterization
474 of Equation 2 clearly underestimated the decay rates. Authors do agree that "soil C
475 turnover is reduced at depth beyond what is expected from environmental controls"
476 (Koven et al., 2013; Guenet et al., 2013). The invoked processes are organic matter
477 protection by association with soil minerals (von Lützow et al., 2006; Rasmussen et al.,
478 2018) and priming effect (Shahzad et al., 2018), which act in interaction. Depth *per se* is
479 not a process-based variable explaining these effects, and the relevant variables still have
480 to be determined.

481 When comparing the different simulation results to measurements, we see that
482 measurements were better reproduced in cropped land, especially when conventional
483 tillage was considered (lowest MSE), then in pasture (Figures 6 and 7). Under cultivation
484 with conventional tillage, the mean bias of the simulation to the OC stock measurements
485 (estimated by the SB indices) was very small except when considering exponential
486 decrease of the decomposition rate coefficients (Figure 7a). The main error was on the
487 ability of the model to reproduce the shape of the data (LCS), except for the reference
488 simulation, the diffusive bioturbation and the exponential decrease of the decomposition
489 rate coefficients. Instead, on those simulations the magnitude of fluctuation among the
490 simulations were furthest from those of measurements (large SDSD). Almost the same
491 trends in the error partitioning (among SB, SDSD and LCS) were observed for cultivation
492 with reduced tillage. The alternative root density functions represented the data better for
493 both conventional and reduced tillage profiles (Figures 7 a and b).

494 While considering pasture, the error distribution change drastically, errors being mainly
495 due to errors on simulating the magnitude of fluctuation among the measurements
496 (SDSD), secondarily to the mean bias of the simulation of the global OC stocks (SB). The
497 models had however a good ability to reproduce the shape of the data as demonstrated by

498 the small LSC values. At last, increasing the belowground contribution of fresh litter
499 provided the best estimation of the OC stock measurements in the pasture (Figure 7c). The
500 strong difference in the model ability to reproduce the OC total stock between cultivation
501 and pasture can be explained by the parametrization of the RothC module that was the
502 same for the two land uses and better suited for cultivation.

503

504 ***Candidate descriptors for deep C dynamics modelling*** - By testing alternative
505 formalisms for the three main processes at the origin of soil C profiles (depth distribution
506 of belowground inputs, soil matter transport and decomposition rates, in these soils with
507 no DOC movement), we could assess the respective weight of each formalism on soil C. We
508 can further discuss the relevant variables for a tentative parameterization. Concerning
509 root inputs, the bi-exponential depth distribution of the roots provides a finer
510 representation of inputs when compared with the mono-exponential, and is more in line
511 with the observation of either biomass (Jobbagy and Jackson, 2000), or young carbon
512 (Balesdent et al., 2018). The single exponential would not bring enough C to the deepest
513 layer, and accordingly would explain deep C stocks only if combined with either strongly
514 reduced carbon decay rates at depth, or carbon input through a diffusion/transport
515 coefficient that would be constant over depth (e.g. Elzein and Balesdent, 1995; Koven et
516 al., 2013). For annual crops, the depth distribution of root input at the annual scale should
517 ideally integrate inputs during plant growth (as eqn. 4 does) and not only final root
518 distribution. At the pluri-annual scale and beyond genotypic drivers, soil moisture
519 (Jobbagy and Jackson, 2000; Balesdent et al., 2018), together with CO₂ partial pressure
520 and fertilization, would be relevant variables of rooting and rhizodeposition. A mass
521 mixing with an intensity decreasing with depth, as is described by equation 8 or would be
522 by an equivalent matrix of transfer of matter in between soil layers, is also in line with
523 observations. Finally, decay rates decrease with depth, but with a smaller gradient than
524 those tested in the parameterization of equation 2. One relevant variable for decay rate
525 modifier would be the carbon input flux itself, acting by priming effect (Cheng et al., 2014;

526 Shazhad et al., 2018). Such a choice would not require additional soil input data for
527 modelling. The second category of variables that affect decay rates is the soil mineralogy
528 expressed either as a weathering indice (Finke et al., 2018), or as secondary minerals
529 (Rasmussen et al., 2017). Soil classification can stand for a proxy of mineralogical
530 properties and may be used to constrain decay rates (Batjes, 2014; Mathieu et al., 2015).
531 But soil mineralogy is not static (Basile-Doelsch et al., 2015), and may evolve gradually
532 with pedogenesis (Finke et al., 2018). This evolution of minerals naturally drove the build-
533 up of the slow component of SOM over the Holocene, but may also be very rapid under
534 man's pressure: agriculture alkalize acidic soils by liming, or reversely acidify soils by N-
535 fertilization and removal of bases (Guo et al., 2013); global N deposition as well acidifies
536 world soils. Due to these major interactions between the dynamics of carbon and minerals,
537 coupled model of carbon and pedogenesis as proposed in this study represent a step
538 forward. According to the variables we listed, it is furthermore expected that future
539 carbon depth distribution will be affected by changes in landuse, precipitation and NPP.

540

541 3.2 Impact of climate, land use and agricultural practices on OC depth distribution:
542 variability among OC-VGEN settings

543 3.2.1 Impact of land use and agricultural practice change on soil OC storage

544 Agriculture with conventional tillage was used for the spin up scenario thus considered as
545 a reference scenario in this analysis. While simulating 72 years of this land use, small
546 oscillations of climate and C inputs as well as a change of ploughing depth from year 2000
547 occurred. These small changes resulted in small fluctuations of the total OC stock observed
548 whatever the considered formalisms or parameters (Figure 8a). While considering deep
549 OC stocks, the different simulations started to deviate from year 2000 (Figure 8d), most
550 probably due to the more superficial ploughing depth that was applied from that date. For
551 deep OC stocks, the reference model and diffusive bioturbation simulations followed the
552 trend observed for the total OC stocks. The alternative above/below ground organic input

553 and the alternative root density function models decreased those stocks by 3.5 % and
554 2.5 % respectively. The depth dependent decomposition rate coefficient simulated a 2.6 %
555 increase of deep OC stocks compared to the reference model. These evolutions are in
556 agreement with the results discussed in the previous section. The depth dependent
557 decomposition rate coefficient increased the OC depth accumulation and thus
558 counteracted the effect of the shallower ploughing on the OC input to the soil. On the
559 opposite, the decrease of the above/belowground ratio of fresh organic matter and the
560 change of root ground formalisms decreased the deep OC stocks.

561 For 10 years of reduced tillage (from year 2000), no differences with the conventional
562 tillage were simulated for the total OC stocks (Figure 8b), while, when considering only
563 deep OC, the deviation among different models became more pronounced. The deep OC
564 stocks simulated by the model with depth dependent decomposition rate coefficient
565 followed more or less the same trend as the total OC stocks, while, for all the other
566 simulations, the deep OC stocks decreased from years after 2000. This decrease reached
567 3 % by the year 2011 for the reference and diffusive bioturbation models, 5 % for the
568 alternative root growth formalisms and up to 10 % for the increased above/below ground
569 input model (Figure 8e). These results showed that a further shallowing of the ploughing
570 depth increased the trends observed after the year 2000 in the case of the agriculture with
571 conventional tillage. Reduced tillage did not increase the total OC stock compared to
572 conventional tillage. While considering the upper 30 cm, a slight increase ranging from 0
573 to 9 % was observed. Most experiments on reduced tillage in the literature were
574 conducted on durations ranging from 0 to 15 years and thus comparable to the
575 experiment considered in this study. Recent meta-analysis (Baker et al., 2007; Bai et al.,
576 2018) described no significant change in total OC stock with reduced tillage but a change
577 in soil OC distribution comparable to that obtained in this study. Dimassi et al. (2014)
578 attributed this difference to differences in soil climate (water content notably) due to the
579 tillage practices. Our modelling approach could not reproduce such a difference in soil

580 climate due to tillage reduction; the observed changes in OC stocks were mainly due to
581 change in mixing depth and intensity.

582 For pasture, all the simulations resulted in an increase of 30 to 40 % of total OC stocks
583 after 72 years (Figure 8 c). This increase was more marked while considering the upper 30
584 cm OC stock with an increase ranging from 60 to 90% depending on the model considered.
585 Poeplau et al. (2011) estimated a $100 \pm 20\%$ increase in upper 30 cm stock of soils after
586 grassland establishment in temperate regions while the Guo and Gifford (2002) meta-
587 analysis, depicted only a 19% increase. Our modelling approach provided a value closer to
588 that of Poeplau et al. (2011). For deep OC stocks (30-120 cm), the situation was more
589 complex. Only the decrease of above ground input simulated an increase of the deep OC
590 stock by about 15 %. The reference model as well as diffusive bioturbation and depth
591 dependent decomposition rate coefficient models simulated no changes of deep OC stocks
592 over the 72 years. Finally, both alternative root density function models simulated a
593 decrease in deep OC stocks ranging from 3 to 7 % after 72 years, the largest decrease
594 being, as expected, for the Jackson et al (1996) formalism (Figure 8f).

595 3.2.2 Impact of two climate change scenarios by the years 2100 on the soil OC storage
596 simulations for three different land use and agricultural practice modalities

597 For cropped profiles, all of the considered formalisms/parametrisations simulated an
598 increase of the total OC storage ranging from 0 to 3 % at the year 2100 (Figures 9 a and b)
599 and up to the 6 % for the depth dependent decomposition rate coefficient simulation. No
600 significant differences (<2 %) were observed between conventional and reduced tillage in
601 terms of simulated OC stocks. For the pasture, the simulations predicted a larger total OC
602 stock increase ranging from 9 to 11% at the year 2100 (Figure 9c).

603 Considering the two IPCC scenarios, the standard deviation of the simulated OC stocks
604 between RPC8.5 and RPC2.5 ranged from 0 to 3 %, as for cropland, whatever the
605 considered model version.

606 For deep OC stocks (30-120cm), the situation was once again more complex. The increase
607 of above/below ground ratio of fresh organic input led to a decrease of the deep OC
608 stock by 4 and 11 % for conventional and reduced tillage respectively, as well as the use of
609 an alternative root density function (Zeng, 2001) although to a lesser extent (3 % for both
610 plots). In contrast, the model with depth dependent decomposition rate coefficients
611 increased the deep OC stock to a maximum of 8 % for both cropped plots. The reference
612 model and diffusive bioturbation did not induce a significant change over the simulated
613 period. On cropped profiles, the variations of deep OC stocks related to the formalisms/
614 parameters used in the model were larger than that of total OC stocks (Figures 9d and e)
615 and were more marked for shallower tillage, while the effect of IPCC scenarios stayed in
616 the range of 3 %. For pasture, most of the simulations predicted an increase in deep OC
617 stocks, with the exception of the simulation with Jackson et al. (1996)'s root density
618 function that resulted in a slight decrease of the deep OC stock. The maximum increases of
619 6 to 9 % for RCP2.6 and RCP8.5 respectively were simulated by the model with higher
620 below ground fresh organic input (Figure 9f). The effect of IPCC scenarios again produced
621 changes in the deep OC stocks ranging from 0 to 3 %.

622 Thus, regardless of the land use or tillage practices, variabilities in the simulated total OC
623 stocks induced by different soil process formalisms/parameters and by the different
624 forcing scenarios (RCP8.5 and RCP2.6) were of same order of magnitude (Figures 9a to c).
625 When considering the deep OC stocks (30-120 cm), the variability induced by the choice of
626 processes/formalisms used was dominant (Figures 9d to f), showing that efforts on
627 calibrating the deep OC transfer processes are needed.

628 Other studies projecting OC stocks over the 21st century only considered the upper 30 cm
629 of the soil (e.g., Smith et al., 2005; Lugato et al., 2014; Wiesmeier et al., 2016). In this study,
630 by introducing new soil processes and the uncertainty related to their knowledge, we
631 showed that the simulated behaviour of deep OC differs substantially from that of top soil
632 OC stocks. We showed that while for the total OC stocks (as well as top 30 cm OC stocks)

633 an increase could be projected considering the suggested climate change scenarios; both
634 an increase and a decrease in deep OC stock are possible over the coming century
635 depending on the formalism/parameter considered in the simulation.

636

637 **Conclusion**

638 In this paper, we proposed the first fully modular OC depth distribution model,
639 called OC-VGEN that was shown to be efficient for testing the effect of different numerical
640 representations soil processes on OC depth distribution. We demonstrated that the OC-
641 VGEN model include processes that are crucial at a decadal to a century time scale for
642 modelling soil OC stock evolution in Luvisols, notably explicit transfer of water and
643 temperature although only partially for water transfer that remains only indirectly taken
644 into consideration since soil moisture deficit is not directly derived from soil water
645 content at different depths. In addition, transfer of DOC was not considered in this model,
646 since DOC is negligible in the type of soil considered. Nevertheless this process should be
647 added if other soil types as podzols for which this process is dominant had to be modelled.
648 The development of the model under the VSoil modelling platform should ease this
649 implementation.

650 For the numerical representations tested, namely root depth distribution, bioturbation
651 and OC decomposition rate coefficients, we showed that the simulated OC depth-
652 distribution (below 30 cm) was very dependent on the tested formalisms/parameters,
653 while the total soil OC stocks was not. We showed that the use of different soil processes
654 formalisms/parameters had a larger impact on deep OC stock prediction than that of
655 forcing scenarios tested. These forcing scenarios were nevertheless chosen as the extreme
656 cases in the range of possibilities for both land use and climate change. These results
657 demonstrate the need of further calibration of soil processes responsible for the building
658 of deep OC stock in soils. These first results strongly suggest the need for a bioturbation
659 process progressively decreasing with depth and decay rates also decreasing with depth,
660 but with a smaller gradient than the one tested.

661 We proposed here a first modelling approach for OC stock estimation considering most
662 soil processes and their feedbacks. Our study demonstrated that, due to a limited
663 knowledge, considering soil processes added a lot of uncertainties on the soil OC stock

664 projections, notably for the deep soil OC, and thus more effort should be done in
665 evaluating the most reasonable combination of formalisms for soil processes and their
666 parametrization. To do so, this work should be extended to different soil types under
667 different climates in which the hierarchy of the processes could be different, thus allowing
668 better conclusions on the formalisms to be chosen for the different soil processes. Future
669 research with models such as OC-VGEN should especially focus on the above to below
670 ground fresh organic input ratio and on depth-dependent OC decomposition rate
671 coefficients, since OC-VGEN is the most sensitive to these formalisms/parameters.
672 Combining modelling and isotopic tracing approaches, by introducing the isotopes in the
673 models could allow overcoming this limit.

674

675 **Acknowledgement**

676 This research was conducted in the framework of the Agriped project (ANR-10-BLANC-
677 605) and the DeDyCas project (ANR 14-CE01-0004) supported by the French National
678 Research Agency (ANR) and the ASSESS project (ERANETMED2-72-209 ASSESS).

679 S. Keyvanshokouhi received a PhD grant from the French National Institute for
680 Agricultural Research (INRA) and the French agency for environment and energy
681 (ADEME). The authors are grateful to INRA of Mons-en-Chaussee (France) for providing
682 the access to their long-term experimental site and the associated data, to B. Davis for
683 supplying reconstructed temperature and precipitation time series, to Meteo France for
684 providing climatic data from the SAFRAN Grid for the studied site.

References

- Bai, Z., Caspari, T., Ruiperez Gonzalez, M., Batjes, N.H., Mäder, P., Bünemann, E.K, de Goede, R., Brussaard, L., Xu, M., Santos Ferreira, C.S., Reintam, E., Fan, H., Mihelič, R., Glavan, M., Tóth, Z., 2018. Effects of agricultural management practices on soil quality: A review of long-term experiments for Europe and China. *Agriculture, Ecosystems & Environment*, 265, 1-7.
- Baisden, W. T., Amundson, R., Brenner, D. L., Cook, A. C., Kendall, C., Harden, J. W., 2002. A multiisotope C and N modeling analysis of soil organic matter turnover and transport as a function of soil depth in a California annual grassland soil chronosequence. *Global Biogeochemical Cycles*, 16, 1135. doi:10.1029/2001GB001823
- Baker, J. M., Ochsner, T. E., Venterea, R. T., Griffis, T. J., 2007. Tillage and soil carbon sequestration-What do we really know? *Agriculture, Ecosystems and Environment*, 118, 1-5. doi:10.1016/j.agee.2006.05.014
- Balesdent, J., Basile-Doelsch, I., Chadoeuf, J., Cornu, S., Derrien, D., Fekiacova, Z., Hatté, C, 2018. Atmosphere-soil carbon transfer as a function of soil depth. *Nature*, 559, 599–602. doi:10.1038/s41586-018-0328-3
- Basile-Doelsch, I., Balesdent, J., Rose, J. 2015. Are interactions between organic compounds and nanoscale weathering minerals the key drivers of carbon storage in soils? *Environmental Science & Technology* 49, 3997–3998
- Batjes, N., 2014. Total carbon and nitrogen in the soils of the world. *European Journal of Soil Science*, 65, 4-21.
- Boizard, H., Yoon, S. W., Leonard, J., Lheureux, S., Cousin, I., Roger-Estrade, J., Richard, G., 2013. Using a morphological approach to evaluate the effect of traffic and weather conditions

- on the structure of a loamy soil in reduced tillage. *Soil and Tillage Research*, 127, 34-44.
doi:10.1016/j.still.2012.04.007
- Braakhekke, M. C., Beer, C., Hoosbeek, M. R., Reichstein, M., Kruijt, B., Schrumpf, M., Kabat, P.,
2011. SOMPROF: A vertically explicit soil organic matter model. *Ecological Modelling*,
222, 1712-1730. doi:10.1016/j.ecolmodel.2011.02.015
- Brimo, K., Garnier, P., Lafolie, F., Séré, G., Ouvrard, S., 2018. In situ long-term modeling of
phenanthrene dynamics in an aged contaminated soil using the VSOIL platform. *Science
of the Total Environment*, 619–620, 239–24.
- Camino-Serrano, M., Guenet, B., Luysaert, S., Janssens, I. A. 2018. ORCHIDEE-SOM: Modeling soil
organic carbon (SOC) and dissolved organic carbon (DOC) dynamics along vertical soil
profiles in Europe. *Geoscientific Model Development* 11, 937-957.
- Campbell, E. E., Paustian, K., 2015. Current developments in soil organic matter modeling and
the expansion of model applications: a review. *Environmental Research Letters*, 10,
123004. doi:10.1088/1748-9326/10/12/123004
- Canadell, J., Jackson, R. B., Ehleringer, J. B., Mooney, H. A., Sala, O. E., Schulze, E.-D., 1996.
Maximum rooting depth of vegetation types at the global scale. *Oecologia*, 108, 583-595.
doi:10.1007/BF00329030
- Cannavo, P., Lafolie, F., Nicolardot, B., Renault, P., 2006. Modelling seasonal variations in CO₂ and
N₂O concentrations with a model describing C and N behaviour in the vadose zone.
Vadoze Zone Journal, 5, 990-1004.
- Cassini, C. F., 1750. Composite: Carte de France. Carte de France. Levee par ordre du Roy.
Retrieved from <http://www.davidrumsey.com/xmaps10000.html>

- Cheng, W., Parton, W. J., Gonzalez-Meler, M. A., Phillips, R., Asao, S., McNickle, G. G., Brzostek, E., Jastrow, J. D. 2014, Synthesis and modeling perspectives of rhizosphere priming. *New Phytol.* 2014 Jan;201(1):31-44. doi: 10.1111/nph.12440.
- Coleman, K., Jenkinson, D. S., Crocker, G. J., Grace, P. R., Klír, J., Körschens, M., Poulton, P.R., Richter, D.D., 1997. Simulating trends in soil organic carbon in long-term experiments using RothC-26.3. *Geoderma*, 81, 29-44. doi:10.1016/S0016-7061(97)00079-7
- Davidson, J., Graetz, D., Rao, P., Selim, H., 1978. Simulation of nitrogen movement, transformation and uptake in plant root zone. (1978, Ed.)
- Dimassi, B., Mary, B., Wylleman, R., Labreuche, J., Couture, D., Piraux, F., Cohan, J.-P., 2014. Long-term effect of contrasted tillage and crop management on soil carbon dynamics during 41 years. *Agriculture, Ecosystems & Environment*, 188, 134-146. doi:10.1016/j.agee.2014.02.014
- Elzein, A., Balesdent, J., 1995. Mechanistic Simulation of Vertical Distribution of Carbon Concentrations and Residence Times in Soils. *Soil Science Society of America Journal*, 59, 1328-1335. doi:10.2136/sssaj1995.03615995005900050019x
- Finke, P. A., 2012. Modeling the genesis of luvisols as a function of topographic position in loess parent material. *Quaternary International*, 265, 3-17. doi:10.1016/j.quaint.2011.10.016
- Finke, P. A., Hutson, J. L., 2008. Modelling soil genesis in calcareous loess. *Geoderma*, 145, 462-479. doi:10.1016/j.geoderma.2008.01.017
- Finke, P., Opolot, E., Balesdent, J., Berhe, A. A., Boeckx, P., Cornu, S., Harden, J., Hatté, C., Williams, E., Doetterl, S. 2018. Can SOC modelling be improved by accounting for pedogenesis? *Geoderma*, accepted.

- Gale, M. R., Grigal, D. F., 1987. Vertical root distributions of northern tree species in relation to successional status. *Canadian Journal of Forest Research*, 17, 829-834. doi:10.1139/x87-131
- Guenet, B., Eglin, T., Vasilyeva, N., Peylin, P., Ciais, P., Chenu, C., 2013. The relative importance of decomposition and transport mechanisms in accounting for soil organic carbon profiles. *Biogeosciences*, 10, 2379-2392. doi:10.5194/bg-10-2379-2013
- Guo, J. H., Liu, X.J., Zhang, Y., Shen, J. L., Han, W. X., Zhang, W. F., Christie, P., Goulding, K. W. T., Vitousek, P. M., Zhang, F. S., 2010. Significant Acidification in Major Chinese Croplands *Science*, 327,1008-1010
- Guo, L. B., Gifford, R. M., 2002. Soil carbon stocks and land use change: a meta analysis. *Global Change Biology*, 8, 345-360. doi:10.1046/j.1354-1013.2002.00486.x
- Haddaway, N. R., Hedlund, K., Jackson, L. E., Kätterer, T., Lugato, E., Thomsen, I. K., Jørgensen, H.B., Isberg, P.-E., 2016. How does tillage intensity affect soil organic carbon? A systematic review protocol. *Environmental Evidence*, 5, 1-1. doi:10.1186/s13750-016-0052-0
- He, Y., Trumbore, S.E, Torn, M.S., Harden, J.W., Vaughn, L.J.S., Allison, S.D., Randerso, J.T., 2016. Radiocarbon constraints imply reduced carbon uptake by soils during the 21st century. *Science* 353, 1419-142.
- Hilinski TE (2001) 'Implementation of exponential depth distribution of organic carbon in the CENTURY Model. CENTURY soil organic matter model user's manual.' (Department of Soil and Crop Sciences, Colorado State University: Fort Collins, CO).

- Hutson, J. L., 2003. Leaching Estimation and Chemistry Model: A Process-Based Model of Water and Solute Movement, Transformations, Plant Uptake, and Chemical Reactions in the Unsaturated Zone. Department of Crop and Soil Sciences, Cornell University, Ithaca.
- Jackson, R. B., Canadell, J., Ehleringer, J. R., Mooney, H. A., Sala, O. E., Schulze, E. D., 1996. A global analysis of root distributions for terrestrial biomes. *Oecologia*, 108, 389-411. doi:10.1007/BF00333714
- Jagercikova, M., Evrard, O., Balesdent, J., Lefèvre, I., Cornu, S., 2014. Modeling the migration of fallout radionuclides to quantify the contemporary transfer of fine particles in Luvisol profiles under different land uses and farming practices. *Soil and Tillage Research*, 140, 82-97. doi:10.1016/j.still.2014.02.013
- Janik, L., Spouncer, L., Correll, R., Skjemstad, J., 2002. Sensitivity analysis of the RothC carbon model. National Carbon Accounting System technical report; No. 30. ISSN: 14426838
- Jarvis, N. J., Taylor, A., Larsbo, M., Etana, A., Rosén, K., 2010. Modelling the effects of bioturbation on the re-distribution of ¹³⁷Cs in an undisturbed grassland soil. *European Journal of Soil Science*, 61, 24-34. doi:10.1111/j.1365-2389.2009.01209.x
- Jenkinson, D. S., Coleman, K., 2008. The turnover of organic carbon in subsoils. Part 2. Modelling carbon turnover. *European Journal of Soil Science*, 59, 400-413. doi:10.1111/j.1365-2389.2008.01026.x
- Kobayashi, K., Salam, M. U., 2000. Comparing simulated and measured values using mean squared deviation and its components. *Agron. J.*, 92(2), 345-352, doi:10.2134/agronj2000.922345x
- Koven, C. D., Riley, W. J., Subin, Z. M., Tang, J. Y., Torn, M. S., Collins, W. D., Bonan, G. B., Lawrence, D. M., Swenson, S. C., 2013. The effect of vertically resolved soil biogeochemistry and

alternate soil C and N models on C dynamics of CLM4. *Biogeosciences*, 10, 7109-7131.
doi:10.5194/bg-10-7109-2013

Krinner, G., Viovy, N., Noblet, N., Friedlingstein, P., Ciais, P., 2002. A dynamical global vegetation model for studies of the coupled atmosphere-biosphere system. *Global Biogeochemical Cycles*, 19(GB1015), 1 - 44. DOI: [10.1029/2003GB002199](https://doi.org/10.1029/2003GB002199)

Lafolie, F., Cousin, I., Marron, P.-A., Mollier, A., Pot, V., Moitrier, Ni., Moitrier, Na, Nouguier, C., 2014. The "VSOIL" modeling platform. *Rev. For. Fr.* LXVI, hors série 2014 (2014) (ISSN 0035) <https://doi.org/10.4267/2042/56287>

Lal, R., 2004. Soil Carbon Sequestration Impacts on Global Climate Change and Food Security. *Science*, 304, 1623-1627. doi:10.1126/science.1097396

Lorenz, K., Lal, R., 2005. The Depth Distribution of Soil Organic Carbon in Relation to Land Use and Management and the Potential of Carbon Sequestration in Subsoil Horizons. *Advances in Agronomy*, 88, 35-66.
<http://www.sciencedirect.com/science/article/pii/S0065211305880022>

Lugato, E., Panagos, P., Bampa, F., Jones, A., Montanarella, L., 2014. A new baseline of organic carbon stock in European agricultural soils using a modelling approach. *Global Change Biology*, 20, 313-326. doi:10.1111/gcb.12292

Luo, Y., Ahlström, A., Allison, S.D., Batjes, N.H., Brovkin, V., Carvalhais, N., Chappell, A., Ciais, P., Davidson, E.A., Finzi, A., Georgiou, K., Guenet, B., Hararuk, O., Harden, J.W., He, Y., Hopkins, F., Jiang, L., Koven, C., Jackson, R.B., Jones, C.D., Lara, M.J., Liang, J., McGuire, A.D., Parton, W., Peng, C., Randerson, J.T., Salazar, A., Sierra, C.A., Smith, M.J., Tian, H., Todd-Brown, K.E.O., Torn, M., van Groenigen, K.J., Wang, Y.P., West, T.O., Wei, Y., Wieder, W.R., Xia, J., Xu, X., Xu, X., Zhou, T., 2016. Toward more realistic projections of soil carbon

dynamics by Earth system models. *Glob. Biogeochem. Cycles*, 30, 40–56, doi:10.1002/2015GB005239

von Lützow, M., Kögel-Knabner, I., Ekschmitt, K., Matzner, E., Guggenberger, G., Marschner, B., Flessa, H., 2006. Stabilization of organic matter in temperate soils: mechanisms and their relevance under different soil conditions – a review. *European Journal of Soil Science*, 57, 426-445. doi:10.1111/j.1365-2389.2006.00809.x

Minasny, B., Malone, B. P., McBratney, A. B., Angers, D. A., Arrouays, D., Chambers, A., Chaplot, V., Chen, Z.S., Cheng, K., Das, B.S., Field, D.J., Gimona, A., Hedley, C.B., Hong, S.Y., Mandal, B., Marchant, B.P., Martin, M., McConkey, B.G., Mulder, V.L., O'Rourke, S., Richer-de-Forges, A.C., Odeh, I., Padarian, J., Paustian, K., Pan, G., Poggio, L., Savin, I., Stolbovoy, V., Stockmann, U., Sulaeman, Y., Tsui, C.C, Vågen, T.G., van Wesemael, B., Winowiecki, L., 2017. Soil carbon 4 per mille. *Geoderma*, 292, 59-86. doi:10.1016/j.geoderma.2017.01.002

Montagne, D., Cornu, S., Le Forestier, L., Hardy, M., Josière, O., Caner, L., Cousin, I., 2008. Impact of drainage on soil-forming mechanisms in a French Albeluvisol: Input of mineralogical data in mass-balance modelling. *Geoderma*, 145, 426-438. doi:10.1016/j.geoderma.2008.02.005

Nakane, K., 1978. A Mathematical Model of the Behavior and Vertical Distribution of Organic Carbon in Forest Soils: II. a Revised Model Taking the Supply of Root Litter into Consideration. *Japanese Journal of Ecology*, 28, 169-177. doi:10.18960/seitai.28.3_169

Parton, W. J., 1996. The CENTURY model. In *Evaluation of Soil Organic Matter Models*, pp. 283-291. Springer, Berlin, Heidelberg. Retrieved from https://link.springer.com/chapter/10.1007/978-3-642-61094-3_23

- Paustian, K., Andrén, O., Janzen, H. H., Lal, R., Smith, P., Tian, G., [Tiessen](#), H., [Van Noordwijk](#), M., Woomer, P. L., 1997. Agricultural soils as a sink to mitigate CO₂ emissions. *Soil Use and Management*, 13, 230-244. doi:10.1111/j.1475-2743.1997.tb00594.x
- Poeplau, C., Don, A., Vesterdal, L., Leifeld, J., Van Wesemael, B., Schumacher, J., Gensior, A., 2011. Temporal dynamics of soil organic carbon after land-use change in the temperate zone – carbon response functions as a model approach. *Global Change Biology*, 17, 2415-2427. doi:10.1111/j.1365-2486.2011.02408.x
- Post, W. M., Kwon, K. C., 2000. Soil carbon sequestration and land-use change: processes and potential. *Global Change Biology*, 6, 317-327. doi:10.1046/j.1365-2486.2000.00308.x
- Quintana-Seguí, P., Le Moigne, P., Durand, Y., Martin, E., Habets, F., Baillon, MCanellas, C., Franchisteguy, L., Morel, S., 2008. Analysis of Near-Surface Atmospheric Variables: Validation of the SAFRAN Analysis over France. *Journal of Applied Meteorology and Climatology*, 47, 92-107. doi:10.1175/2007JAMC1636.1
- Rasmussen, C., Heckman, K., Wieder, W.R., Keiluweit, M., Lawrence, C.R., Berhe, A.A., Blankinship, J.C., Crow, S.E., Druhan, J.K, Hicks Pries, C.E., Marin-Spiotta, E., Plante, A.F., Schädel, C., Schimel, J.P., Sierra, C.A., Thompson, A., Wagai, R., 2018. Beyond clay: towards an improved set of variables for predicting soil organic matter content. *Biogeochemistry* 137 (3): 297-306. <https://doi.org/10.1007/s10533-018-0424-3>
- Riley, W. J., Maggi, F., Kleber, M., Torn, M. S., Tang, J. Y., Dwivedi, D., Guerry, N., 2014. Long residence times of rapidly decomposable soil organic matter: application of a multi-phase, multi-component, and vertically resolved model (BAMS1) to soil carbon dynamics. *Geosci. Model Dev.*, 7, 1335-1355. doi:10.5194/gmd-7-1335-2014

- Shahzad, T., Rashid, M. I., Maire, V., Barot, S., Perveen, N., Alvarez, G., Mougin C., Fontaine, S. 2018
Root penetration in deep soil layers stimulates mineralization of millennia-old organic
carbon. *Soil Biol. Biochem.*, 124, 150-160.
<https://doi.org/10.1016/j.soilbio.2018.06.010>
- Smith, J., Smith, P., Wattenbach, M., Zaehle, S., Hiederer, R., Jones, R. J., Montanarella, L.,
Rounsevell, M.D.A., Reginster, I., Ewert, F., 2005. Projected changes in mineral soil
carbon of European croplands and grasslands, 1990–2080. *Global Change Biology*, 11,
2141-2152. doi:10.1111/j.1365-2486.2005.001075.x
- Smith, P., Fang, C., Dawson, J. J., Moncrieff, J. B., 2008. Impact of Global Warming on Soil Organic
Carbon. *Advances in Agronomy*, 97, 1-43.
<http://www.sciencedirect.com/science/article/pii/S0065211307000016>
- Tonneijck, F. H., Velthuis, M., Bouten, W., Van Loon, E. E., Sevink, J., Verstraten, J. M., 2016. The
effect of change in soil volume on organic matter distribution in a volcanic ash soil.
European Journal of Soil Science, 67, 226-236. doi:10.1111/ejss.12329
- Vuuren, P., Edmonds, J., Kainuma, M., Riahi, K., Thomson, A., Hibbard, K., Hurtt, G.C., Kram, T.,
Krey, V., Lamarque, J.F., Masui, T., Meinshausen, M., Nakicenovic, N., Smith, S.J., Rose, S.K.,
2011. The representative concentration pathways: an overview. *Climatic Change*, 109, 5-
31. doi:10.1007/s10584-011-0148-z
- Warszawski, L., Frieler, K., Huber, V., Piontek, F., Serdeczny, O., Schewe, J., 2014. The Inter-
Sectoral Impact Model Intercomparison Project (ISI-MIP): project framework.
Proceedings of the National Academy of Sciences of the United States of America, 111,
3228-3232. doi:10.1073/pnas.1312330110

- Wiesmeier, M., Poeplau, C., Sierra, C. A., Maier, H., Frühauf, C., Hübner, R., Kühnel, A., Spörlein, P., Geuß, U., Hangen, E., Schilling, B., von Lützw, M., Kögel-Knabner, I., 2016. Projected loss of soil organic carbon in temperate agricultural soils in the 21st century: effects of climate change and carbon input trends. *Scientific Reports*, 6. doi:10.1038/srep32525
- Wösten, J.H.M., Lilly, A., Nemes, A., Le Bas, C., 1999. Development and use of a database of hydraulic properties of European soils. *Geoderma*, 90, 169–185.
- Xu, X., Liu, W., Kiely, G., 2011. Modeling the change in soil organic carbon of grassland in response to climate change: Effects of measured versus modelled carbon pools for initializing the Rothamsted Carbon model. *Agriculture, Ecosystems & Environment*, 140, 372-381. doi:10.1016/j.agee.2010.12.018
- Zeng, X., 2001. Global Vegetation Root Distribution for Land Modeling. *Journal of Hydrometeorology*, 2, 525-530. doi:10.1175/1525-7541(2001)002%3C0525:GVRDFL%3E2.0.CO;2

Figure captions

Figure 1: Processes involved in the OC depth distribution and the feedbacks between them. DPM: decomposable plant material, RPM: resistant plant material, BIO: biomass, HUM: humus, and IOM: inert organic matter.

Figure 2: Forcing scenarios for the past reconstruction and the spin-up a) precipitation, b) mean temperatures, and c) organic carbon inputs for different land-use and tillage histories. The period ranging from 1940 to the vertical dashed line was used as spin up scenario.

Figure 3: Forcing scenarios for the climate change scenarios over the coming century: anomalies of a) precipitation, b) average temperature obtained with climatic data produced by HadGEM (H), IPSL-CM5A (I) and MIROC-ESM-CH (M) Earth System Models and c) net primary production (NPP) produced by ORCHIDEE. Code 2.6 is used to represent the RCP 2.6 scenarios (greenhouse emissions decreasing after 2020) and 8.5 to represent RCP 8.5 scenarios (emissions continue to rise).

Figure 4: General layout of the simulations.

Figure 5: Differences of simulated OC depth distribution between the reference model and the alternative formalisms/parameters for conventional tillage (M1), reduced tillage (M2) and pasture (M3): a) Jackson et al. (1996) rooting density function, b) Zeng. (2001) rooting density

function, c) bioturbation, d) above/below ground fresh organic input, and e) depth dependent decomposition rate coefficient.

Figure 6: Simulated OC depth distribution in 2011 by the 6 different versions of OC-VGEN model based different formalisms/parameters and measurements for a) the conventional tillage (M1), b) the reduced tillage (M2), and c) the pasture (M3) profiles. Segmented line with error bars depict the measurements and the associated uncertainties. For description of formalism scenarios see Table 2. Units are t C ha⁻¹ per 5 cm-thick layer.

Figure 7: Mean square deviation (MSD) and its components, namely square bias (SB), squared difference between standard deviations (SDSD) and lack of correlation weighted by the standard deviation (LCS) for the OC depth distributions simulated by the 6 model versions compared to measurements for a) conventional tillage (M1), b) reduced tillage (M2) and c) pasture (M3).

Figure 8: Simulated soil OC stock change relative to the initial stock over 72 years, considering 6 soil process formalisms and parameters. a) and d) represent continuous conventional tillage (M1); b) and e) reduced tillage (M2) and c) and f) pasture (M3). Change in the total OC stock is shown in a), b) and c) and in stock below 30 cm in d), e) and f). For description of the formalisms, see Table 2.

Figure 9: Projection of the total soil OC stock over the coming century considering 6 climatic scenarios and 7 OC-VGEN versions differing by their formalism/parameter. a) and d) represent conventional tillage, b) and e) reduced tillage and c) and f) pasture. Blue lines represent the RCP2.6 IPCC climatic scenario and red lines represent the RCP8.5 IPCC climatic scenario for all

the three Earth System Models. For description of the formalisms, see Table 2. Lines represents the average of the three climatic model for each climatic scenario and the coloured areas represent the bandwidths of the simulation results of the three climatic model for a given climatic scenario.

Table captions

Table 1: List of the major processes and corresponding modules used to build OC-VGEN model inside VSoil platform. Some of them were used from the official inventory of VSoil platform (highlighted), while other had to be created either based on modules pre-existing in the literature or completely newly designed (bold).

Table 2: Summary of the scenarios of the different numerical representations (formalisms and parameters) tested on the three Luvisol profiles of pasture and cropped land with conventional and reduced tillage.

Table 3: Description of the study site. M1, M2 and M3 stands for the three studied plots in Mons.

Table 4: OC stocks (t ha⁻¹) simulated at the end of the 72 years simulations with different soil processes formalisms/parameters in OC-VGEN for the three experimental plots.

Table

[Click here to download Table: Keyvanshokouhi_et_al_tables_revised.doc](#)

Table 1: List of the major processes and corresponding modules used to build OC-VGEN model inside VSoil platform. Some of them were used from the official inventory of VSoil platform (highlighted), while other had to be created either based on modules pre-existing in the literature or completely newly designed (bold).

Process		Module	Original model	Reference
Organic matter dynamics		Exponential decay of OC pools	RothC-26.3	Coleman et al. (1997)
Water, gaz and heat transport	Gas transport and balance	Convection-diffusion equation	PASTIS	Cannavo et al. (2006)
	Heat transport and balance	Convection-diffusion equation	PASTIS	Cannavo et al. (2006)
	Water flow and balance	Richard's equation	PASTIS	Cannavo et al. (2006)
	Change in soil hydraulic properties	Hypres pedotransfer function	SoilGen	Finke (2012) after Wösten et al. (1999)
	Water runoff	Removing excess water	LEACHC	Hutson (2003)
Plant development	Plant development	Input file	SoilGen	Finke (2012)
	OC matter input to the ground	Input file	SoilGen	Finke (2012)
	Root development	Exponential root growth	SoilGen	Finke and Hutson (2008)
	Root water uptake		LEACHC	Hutson (2003)
Solid vertical mixing	Bioturbation	Vertical mixing + compartment homogenization	SoilGen	Finke and Hutson (2008)
	Tillage practices	Vertical mixing + compartment homogenization	SoilGen	Finke and Hutson (2008)
Solid mineral balance		Balancing soil characteristics	OC-VGEN	This study

Table 2: Summary of the scenarios of the different numerical representations (formalisms and parameters) tested on the three Luvisol profiles of pasture and cropped land with conventional and reduced tillage.

Scenario name	Land use	Root depth distribution (RDF)	Above/below ground fresh OC ratio	Bioturbation	Decomposition coefficient
Reference setting -Ref	Crop	$RDF(z, t) = R_{max}(t) \exp(-\beta z^2) \cos \frac{\pi z}{2L(t)}$	41/59	Mixing model after SoilGen2.24	$K(z) = K_{0,p} T_T(z) r_{w\tau}(z) r_{sc}(z)$
	Pasture	$RDF(z) = \alpha \cdot e^{-\alpha z}$	58/42		
Alt 1 - RD_Jackson	Crop	$RDF(z) = -\ln(\beta) \cdot \beta^z$	41/59	Mixing model after SoilGen2.24	$K(z) = K_{0,p} T_T(z) r_{w\tau}(z) r_{sc}(z)$
	Pasture		58/42		
Alt 2 - RD_Zeng	Crop	$RDF(z) = \frac{1}{2} (\alpha \cdot e^{-\alpha z} + b \cdot e^{-bz})$	41/59	Mixing model after SoilGen2.24	$K(z) = K_{0,p} T_T(z) r_{w\tau}(z) r_{sc}(z)$
	Pasture		58/42		
Alt 3 - RD_A/B	Crop	$RDF(z, t) = R_{max}(t) \exp(-\beta z^2) \cos \frac{\pi z}{2L(t)}$	90/10	Mixing model after SoilGen2.24	$K(z) = K_{0,p} T_T(z) r_{w\tau}(z) r_{sc}(z)$
	Pasture	$RDF(z) = \alpha \cdot e^{-\alpha z}$	22/78		
Alt 4 - OC_DDCoeff	Crop	$RDF(z, t) = R_{max}(t) \exp(-\beta z^2) \cos \frac{\pi z}{2L(t)}$	41/59	Mixing model after SoilGen2.24	$K(z) = K_{0,p} T_T(z) r_{w\tau}(z) r_{sc}(z) r_z(z)$
	Pasture	$RDF(z) = \alpha \cdot e^{-\alpha z}$	58/42		
Alt 5 - Bioturb	Crop	$RDF(z, t) = R_{max}(t) \exp(-\beta z^2) \cos \frac{\pi z}{2L(t)}$	41/59		
	Pasture	$RDF(z) = \alpha \cdot e^{-\alpha z}$	58/42	$\frac{\partial M_{oc}(z, t)}{\partial t} = D(z) \frac{\partial^2 M_{oc}(z, t)}{\partial z^2}$	$K(z) = K_{0,p} T_T(z) r_{w\tau}(z) r_{sc}(z)$

Table 3: Description of the study site. M1, M2 and M3 stands for the three studied plots in Mons.

Site	Mons
Coordinates	40° 52'01" N – 3° 01'53" E
Elevation	88 m
Mean annual rainfall	680 mm
Mean annual temperature	11°C
History of land use	M1&M2: wheat-corn-sugar beet M3: pasture since 1939
	Not since 1986 under cultivation and 1939 for pasture
History of agricultural practices for cultivated plots	Liming
	Fertilisation
	Tillage
	M1&M2: data available since 1970 M3: no fertilization since 1939
	M1: conventional tillage since 2001 M2: reduced tillage since 2000 sine 2001 M3: last tillage in 1939

Table 4: OC stocks (t ha⁻¹) simulated at the end of the 72 years simulations with different soil processes formalisms/parameters in OC-VGEN for the three experimental plots.

Soil depth in cm	Formalism/parameter	Land use		
		Agriculture conventional tillage (M1)	reduced tillage (M2)	Pasture (M3)
Ecto-organic layer		Initial stock: 0		
		0	0	22
		0	0	22
		0	0	22
		0	0	9
		0	0	21
0-120		Initial stock: 84		
	Ref	85	85	87
	RD_Jackson	85	86	87
	RD_Zeng	85	86	88
	RD_A/B	84	86	107
	OC_DDcoeff	106	107	110
30-120		Initial stock: 50		
	Ref	45	44	41
	RD_Jackson	39	39	39
	RD_Zeng	40	39	40
	RD_A/B	38	36	47
	OC_DDcoeff	69	68	64
	Bioturb	47	46	43

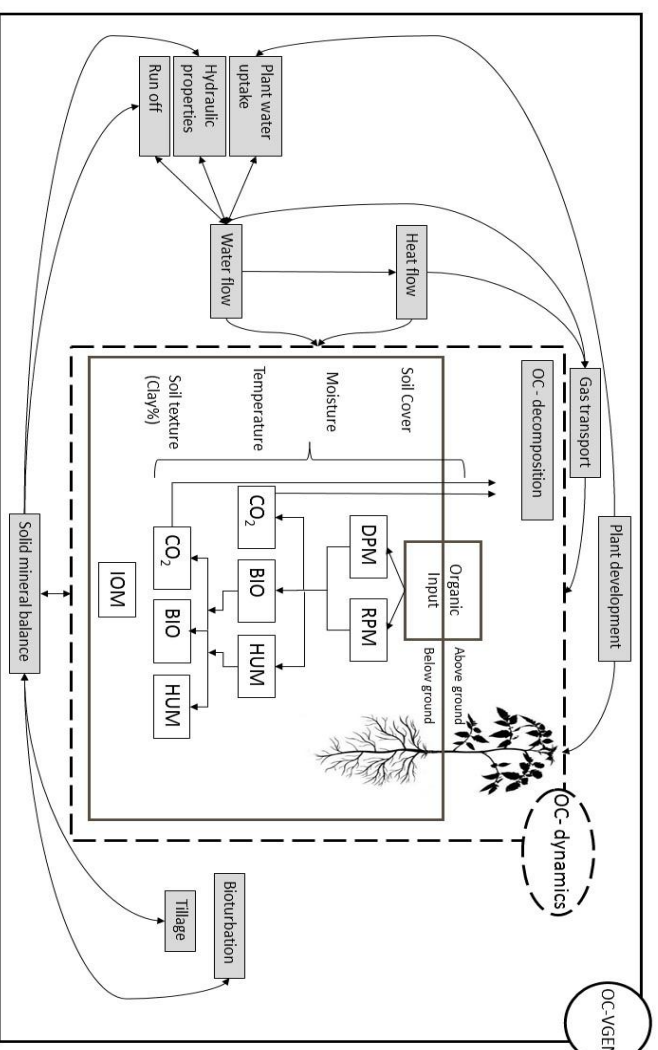


Figure 1: Processes involved in the OC depth distribution and the feedbacks between them. DPM: decomposable plant material, RPM: resistant plant material, BIO: biomass, HUM: humus, and IOM: inert organic matter.

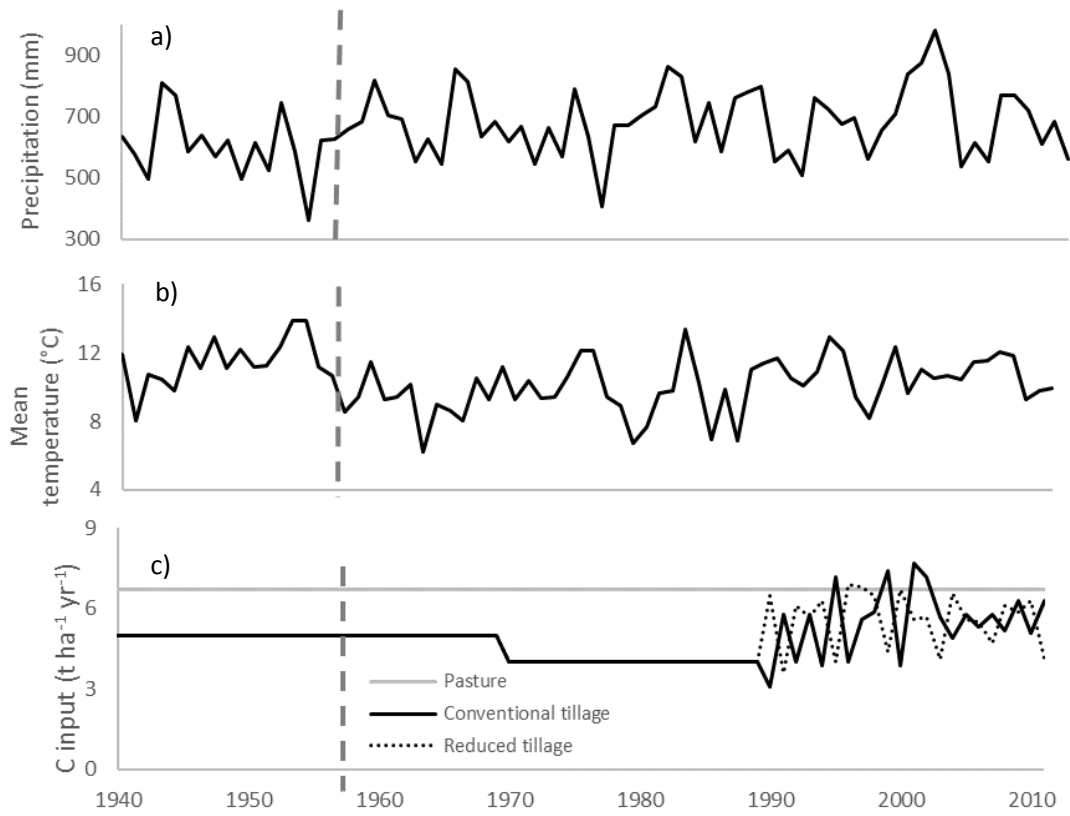


Figure 2: Forcing scenarios for the past reconstruction and the spin-up a) precipitation, b) mean temperatures, and c) organic carbon inputs for different land-use and tillage histories. The period ranging from 1940 to the vertical dashed line was used as spin up scenario.

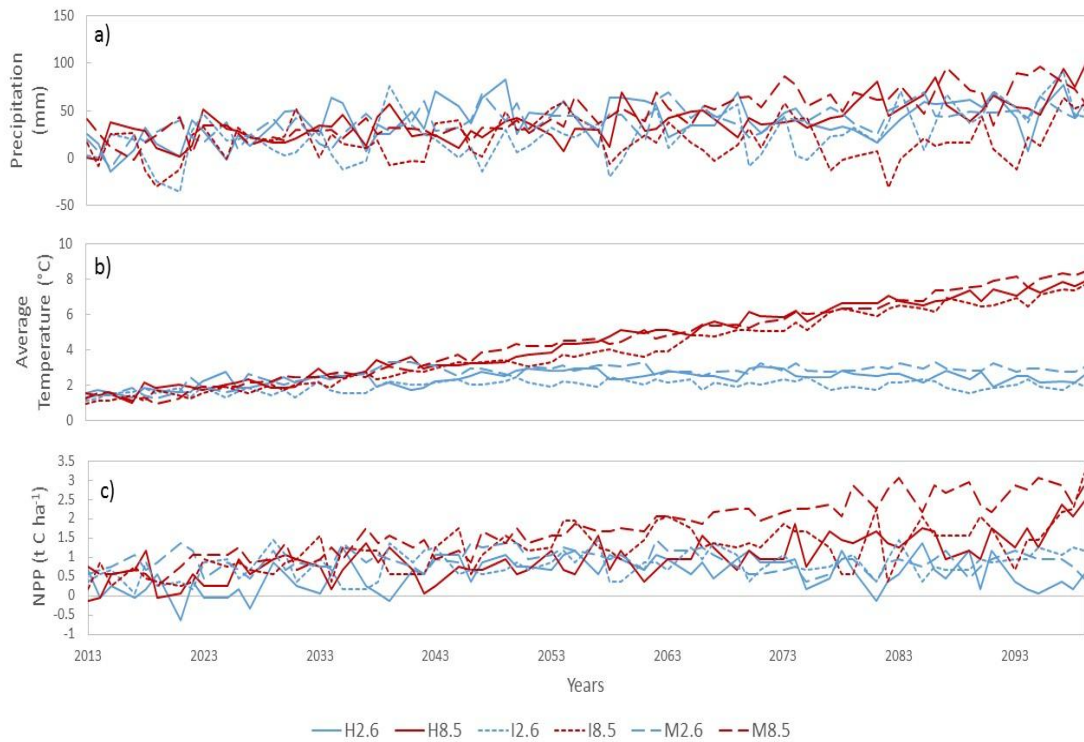


Figure 3: Forcing scenarios for the climate change scenarios over the coming century: anomalies of a) precipitation, b) average temperature obtained with climatic data produced by HadGEM (H), IPSL-CM5A (I) and MIROC-ESM-CH (M) Earth System Models and c) net primary production (NPP) produced by ORCHIDEE. Code 2.6 is used to represent the RCP 2.6 scenarios (greenhouse emissions decreasing after 2020) and 8.5 to represent RCP 8.5 scenarios (emissions continue to rise).

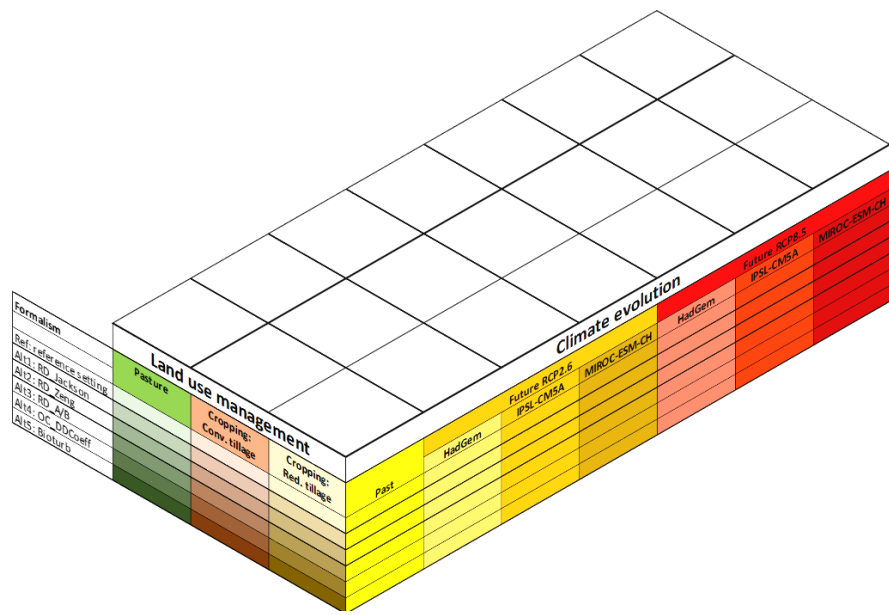


Figure 4: General layout of the simulations.

Figure

[Click here to download Figure: Keyvanshokouhi_et_al_fig5to8_revised.doc](#)

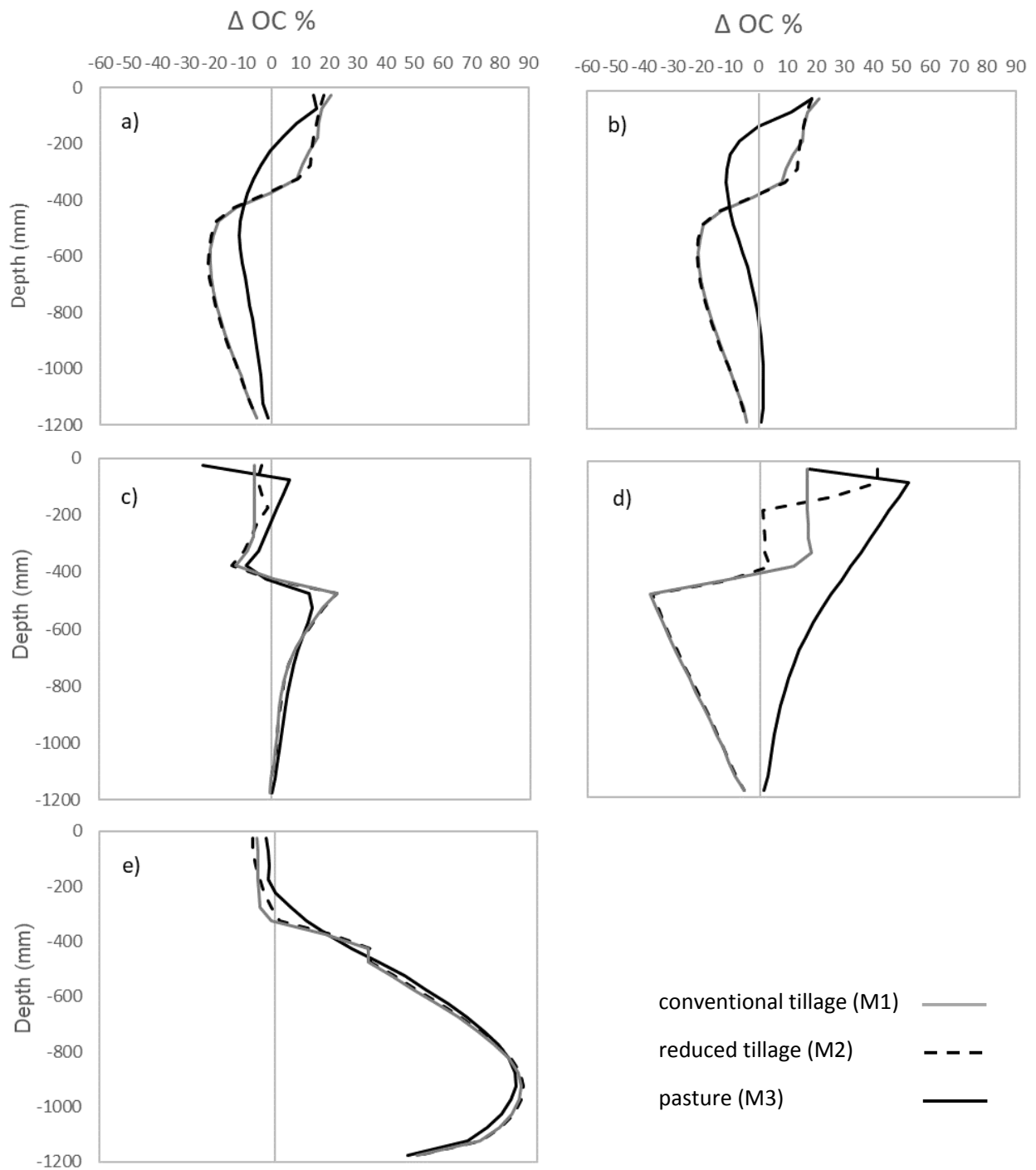


Figure 5: Differences of simulated OC depth distribution between the reference model and the alternative formalisms/parameters for conventional tillage (M1), reduced tillage (M2) and pasture (M3): a) Jackson et al. (1996) rooting density function, b) Zeng. (2001) rooting density function, c) bioturbation, d) above/below ground fresh organic input, and e) depth dependent decomposition rate coefficient.

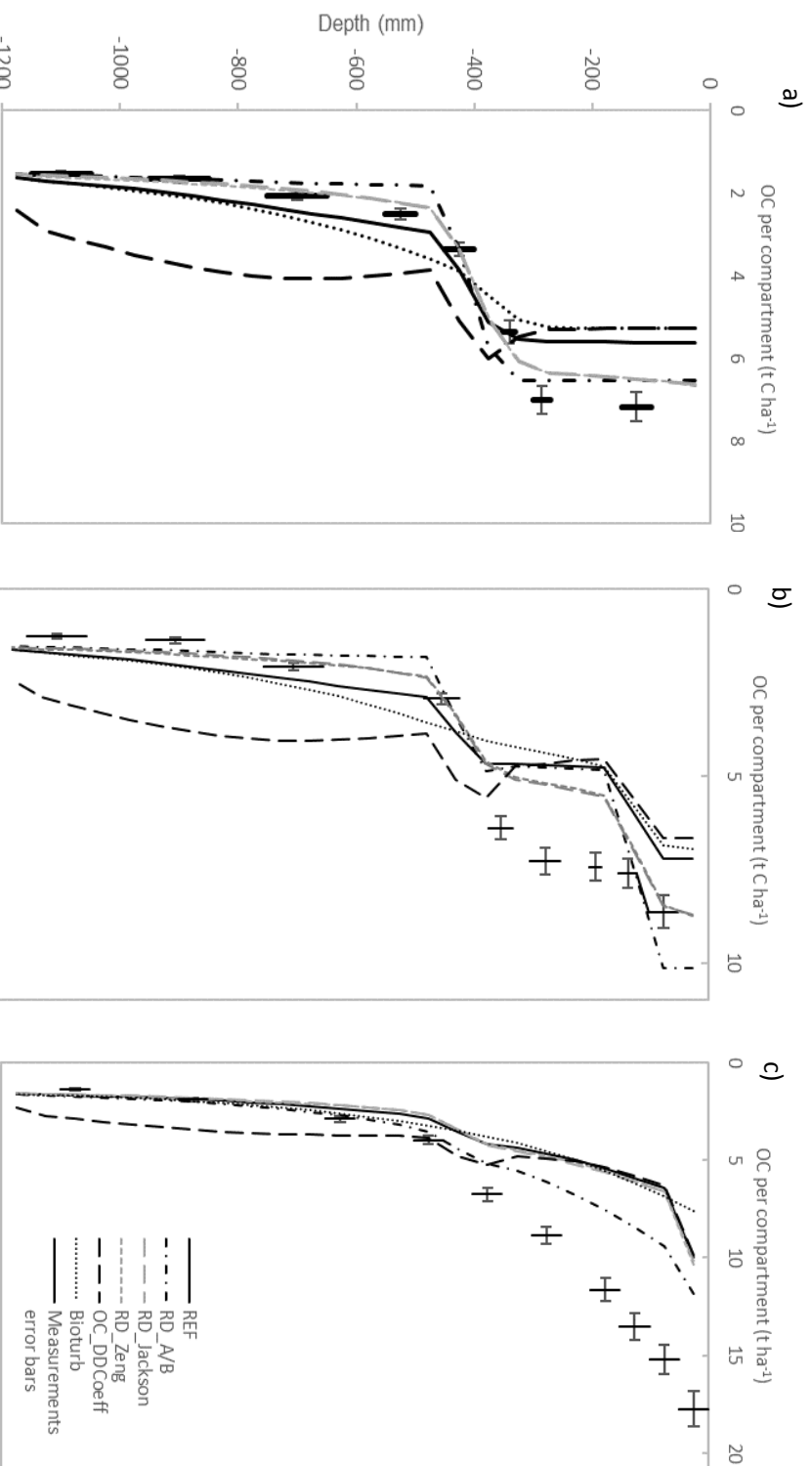


Figure 6: Simulated OC depth distribution in 2011 by the 6 different versions of OC-VGEN model based different formalisms/parameters and measurements for a) the conventional tillage (M1), b) the reduced tillage (M2), and c) the pasture (M3) profiles. Segmented line with error bars depict the measurements and the associated uncertainties. For description of formalism scenarios see Table 2. Units are t C ha⁻¹ per 5 cm-thick layer.

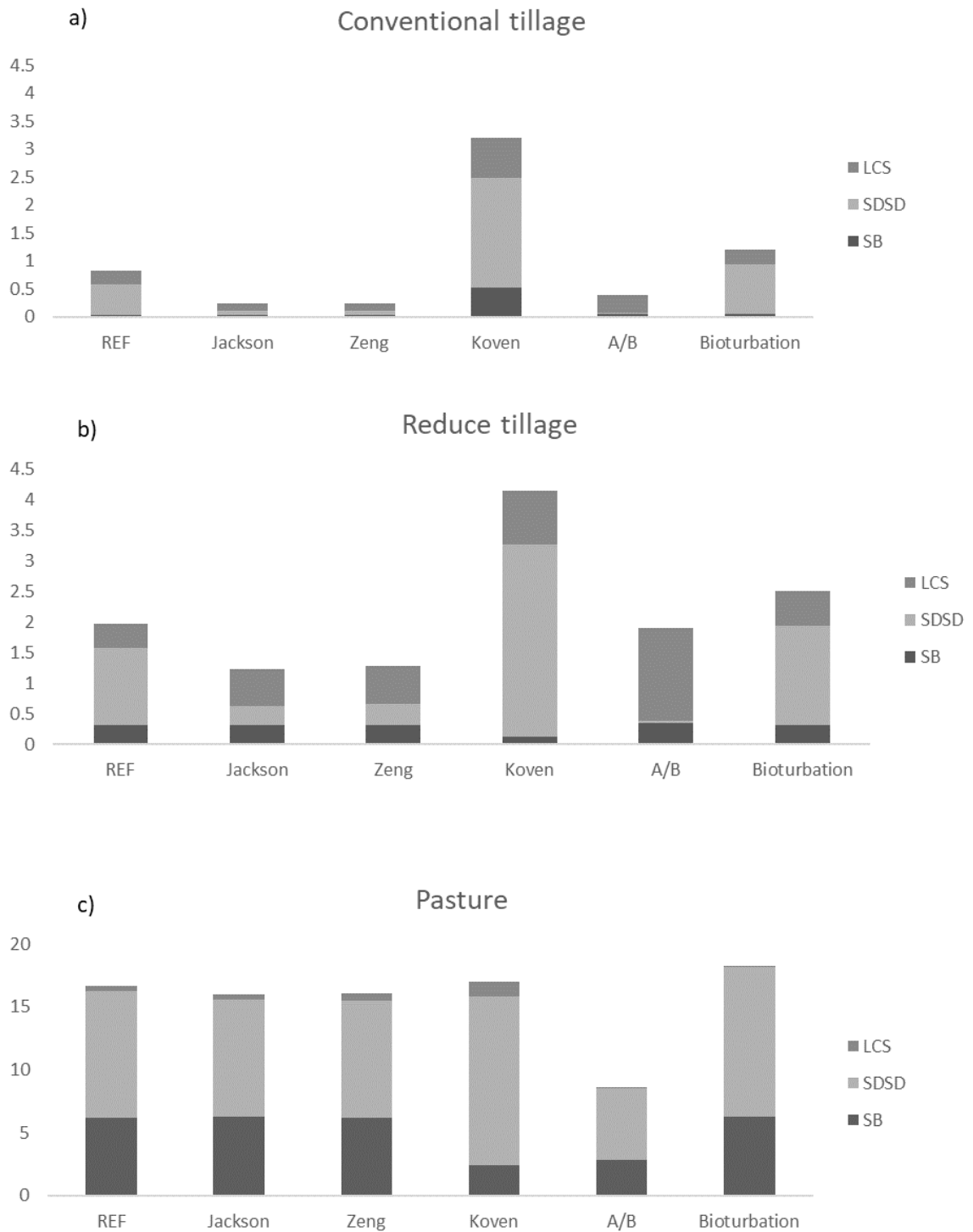


Figure 7: Mean square deviation (MSD) and its components, namely square bias (SB), squared difference between standard deviations (SDSD) and lack of correlation weighted by the standard deviation (LCS) for the OC depth distributions simulated by the 6 model versions compared to measurements for a) conventional tillage (M1), b) reduced tillage (M2) and c) pasture (M3).

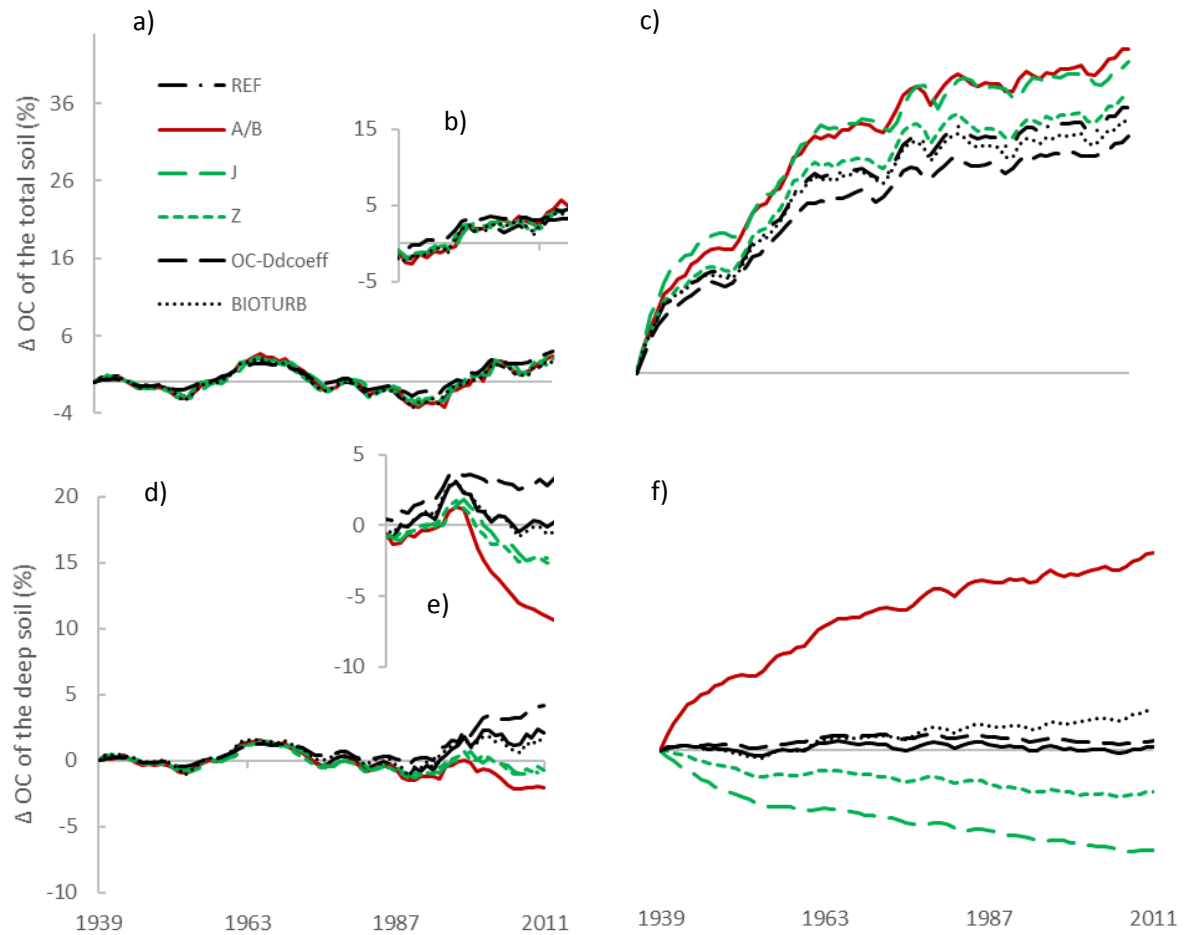


Figure 8: Simulated soil OC stock change relative to the initial stock over 72 years, considering 6 soil process formalisms and parameters. a) and d) represent continuous conventional tillage (M1); b) and e) reduced tillage (M2) and c) and f) pasture (M3). Change in the total OC stock is shown in a), b) and c) and in stock below 30 cm in d), e) and f). For description of the formalisms see Table 2.

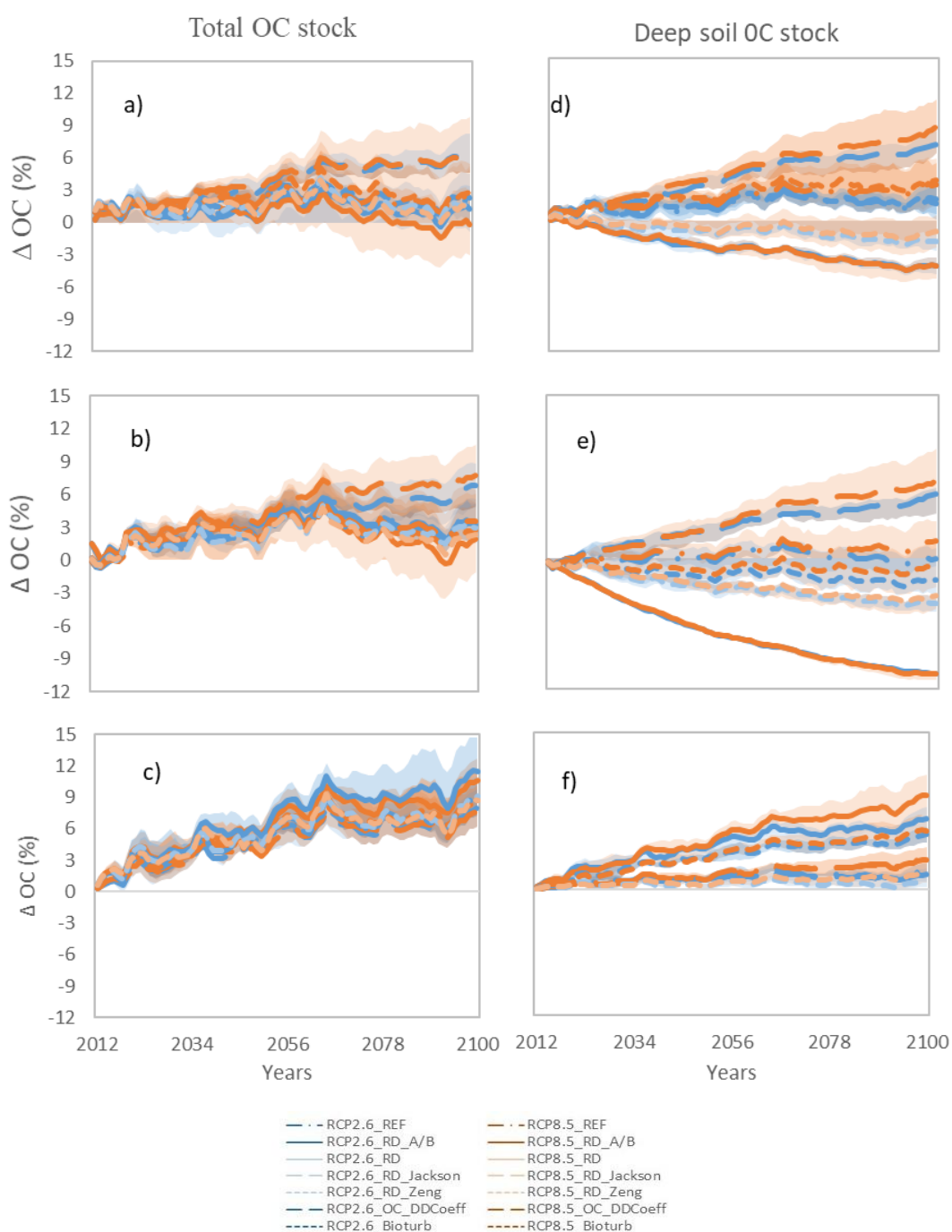


Figure 9: Projection of the total soil OC stock over the coming century considering 6 climatic scenarios and 7 OC-VGEN versions differing by their formalism/parameter. a) and d) represent conventional tillage (M1), b) and e) reduced tillage (M2) and c) and f) pasture (M3). Blue lines represent the RCP2.6 IPCC climatic scenario and red lines represent the RCP8.5 IPCC climatic scenario for all the three Earth System Models. For description of the formalisms, see Table 2. Lines represents the average of the three climatic model for each climatic scenario and the coloured areas represent the bandwidths of the simulation results of the three climatic model for a given climatic scenario.